Weierstraß–Institut
für Angewandte Analysis und Stochastik

im Forschungsverbund Berlin e.V.

Simulation of monolithic microwave integrated circuits

Georg Hebermehl[1] , Rainer Schlundt[1],

Horst Zscheile[2] , Wolfgang Heinrich[2]

submitted: 19th April 1996

[1] Weierstrass Institute for Applied Analysis and Stochastics
Mohrenstraße 39
D – 10117 Berlin
Germany

[2] Ferdinand–Braun–Institut für Höchstfrequenztechnik
Rudower Chaussee 5
D – 12489 Berlin
Germany

Preprint No. 235
Berlin 1996

1991 Mathematics Subject Classification. Microwave device, three–dimensional simulation, scattering matrix, Maxwellian equations, finite–volume method, finite–difference method, eigenvalue problem, system of simultaneous linear equations.
Key words and phrases. 35Q60, 35L20, 65N22, 65F10, 65F15.

e–mail: hebermehl@wias-berlin.de, schlundt@wias-berlin.de, ULR: http://hyperg.wias-berlin.de
e–mail: zscheile@fbh.fta-berlin.de, heinrich@fbh.fta-berlin.de, ULR: http://www.fta-berlin.de.

Edited by
Weierstraß–Institut für Angewandte Analysis und Stochastik (WIAS)
Mohrenstraße 39
D — 10117 Berlin
Germany

Fax: + 49 30 2044975
e–mail (X.400): c=de;a=d400-gw;p=WIAS-BERLIN;s=preprint
e–mail (Internet): preprint@wias-berlin.de

Abstract

The electric properties of monolithic microwave integrated circuits can be described in terms of their scattering matrix using Maxwellian equations. The corresponding three-dimensional boundary value problem of the Maxwellian equations can be solved by means of a finite-volume scheme in the frequency domain. This results in a two-step procedure: a time and memory consuming eigenvalue problem for non-symmetric matrices and the solution of a large-scale system of linear equations with indefinite symmetric matrices.

Contents

List of Figures

1 Introduction

The design of monolithic microwave integrated circuits (MMIC) requires efficient CAD tools in order to avoid costly and time-consuming redesign cycles. Commonly, network-oriented methods are used for this purpose. With increasing frequency and growing packaging density, however, the coupling effects become critical and the simple low-frequency models fail. Thus, field-oriented simulation methods become an indispensable tool for circuit design. Figure 1 illustrates the principal structure under investigation. Since the electric properties are described in terms of the scattering matrix, transmission-line sections have to be attached at the ports. This defines propagation constants and mode patterns required for scattering matrix calculation. Typical line structures are planar lines (microstrip, coplanar waveguide), coaxial lines, or rectangular waveguides.

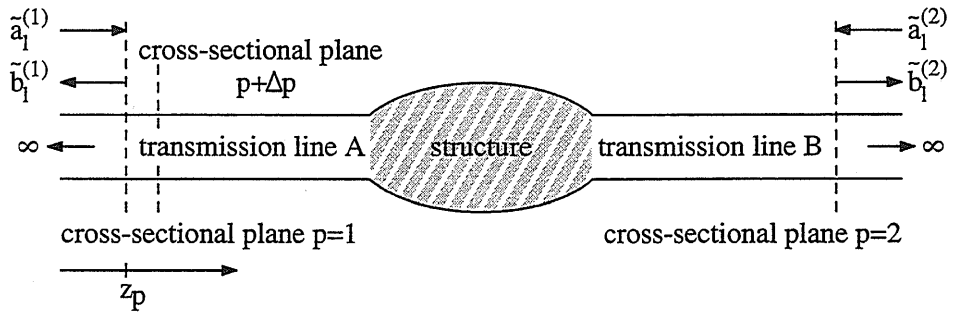

Figure 1: Structure under investigation

The scattering matrix describes the structure in terms of wave modes at the ports [2], [3], [1], which can be computed from the electromagnetic field.
Maxwellian equations are a set of fundamental equations describing all macroscopic electromagnetic phenomena. A three-dimensional boundary value problem can be formulated using the Maxwellian equations in order to compute the electromagnetic field.
The application of the finite-volume method to the three-dimensional boundary value problem for the Maxwellian equations results in the so-called **F**inite-**D**ifference method in the **F**requency **D**omain (FDFD). The field of applications, the advantages of this method, and a comparison to other methods are described in [1].
The program package F3D (Finite Differenzen dreidimensional) [3], [1]

allows to simulate the electromagnetic field of nearly arbitrary shaped structures.
The three-dimensional boundary region is a rectangular box, in its simplest case. This box is subdivided into elementary rectangular cells using a three-dimensional non-equidistant grid. The number of cells determines the order of the resulting matrix equations.
The numerical solution of the boundary value problem is very time-consuming and the storage requirements are high. The most time-consuming parts of the simulation are the computation of eigenvalues and eigenvectors and the solution of linear algebraic equations. Numerical improvements for the simulation of monolithic microwave integrated circuits are described in [4].
In the following we will describe the problem and the finite-volume method for the solution of the three-dimensional boundary value problem.

2 Scattering Matrix

The structures under investigation can be described as an interconnection of infinitely long transmission lines, e.g. waveguides, which must be longitudinally homogeneous. Cross-sectional planes $p = 1$ and $p = 2$ (see Figure 1) are defined on the transmission lines.
The junction of the transmission lines may have an arbitrary structure.
The complex generalized scattering matrix S describes the energy exchange and phase relation between all outgoing modes $\tilde{b}_l^{(p)}$ and all incoming modes $\tilde{a}_l^{(p)}$.
In general, the scattering matrix is of infinite order. But, the order of the scattering matrix S is limited to the order $m_{\bar{s}}$ if on each waveguide only a finite number of modes is considered. That is possible because the energy of the complex and evanescent modes decreases exponentially with the distance from the connecting structure. These modes can be neglected within the limit of accuracy. Only a finite number of modes is able to propagate and have to be taken into consideration.

$$S = \begin{pmatrix} S_{11} & S_{12} & \cdots & S_{1m_{\overline{s}}} \\ S_{21} & S_{22} & \cdots & S_{2m_{\overline{s}}} \\ \cdots & \cdots & \cdots & \cdots \\ S_{m_{\overline{s}}1} & S_{m_{\overline{s}}2} & \cdots & S_{m_{\overline{s}}m_{\overline{s}}} \end{pmatrix} = (S_{\rho,\sigma}), \quad \rho,\sigma = 1(1)m_{\overline{s}}. \tag{1}$$

Let be $m^{(p)}$ the number of modes which have to be taken into account on the cross-sectional plane p. Let be $\overline{p}$ the number of cross-sectional planes. Then we have a total sum $m_{\overline{s}}$ of all modes which have to be taken into account:

$$m_{\overline{s}} = \sum_{p=1}^{\overline{p}} m^{(p)}. \tag{2}$$

The modes on a cross-sectional plane p are numbered with l. Then the indices ρ (and σ) are related to the mode l in the following way

$$\rho = l + \sum_{q=1}^{p-1} m^{(q)}. \tag{3}$$

The scattering matrix S can be extracted from the orthogonal decomposition of the electric field at two neighboring cross-sectional planes on each waveguide for a number of linear independent excitations. Therefore, we need the electric field.
The electric field is computed using a boundary value problem for the Maxwellian equations. The boundary value problem is formulated in the next section.
The computation of the coefficients of the scattering matrix is treated in [4].

3 The Boundary Value Problem

The following assumptions are applied for the structure (see Figure 1).

- The waveguides are longitudinally homogeneous and infinitely long.
- The waveguides and the structure are shielded by electric or magnetic walls.
- The waveguides and the enclosures are cut at cross-sectional planes p.

- The tangential electric or the tangential magnetic field is known on the whole surface.

This means that a three-dimensional boundary value problem of the Maxwellian equations is formulated:

Differential form		Integral form	
$\nabla \times \vec{H}$	$= \vec{J} + \frac{\partial \vec{D}}{\partial t}$,	$\oint_{\partial\Omega} \vec{H} \cdot d\vec{s}$	$= \int_{\Omega} (\vec{J} + \frac{\partial \vec{D}}{\partial t}) \cdot d\vec{\Omega},$
$\nabla \times \vec{E}$	$= -\frac{\partial \vec{B}}{\partial t}$,	$\oint_{\partial\Omega} \vec{E} \cdot d\vec{s}$	$= \int_{\Omega} (-\frac{\partial \vec{B}}{\partial t}) \cdot d\vec{\Omega},$
$\nabla \cdot \vec{D}$	$= \rho$,	$\oint_{\Omega} \vec{D} \cdot d\vec{\Omega}$	$= \int_{V} \rho \, dV,$
$\nabla \cdot \vec{B}$	$= 0$,	$\oint_{\Omega} \vec{B} \cdot d\vec{\Omega}$	$= 0$.

(4)

The first Maxwellian equation is a generalization of Ampère's law by the addition of the displacement current density $\frac{\partial \vec{D}}{\partial t}$. The second Maxwellian equation is Faradays theorem of induction. The two divergence equations of (4) correspond to Gauss' flux laws.
The differential and the integral form of the Maxwellian equations are related by Stokes' theorem and Gauss' theorem.
In this paper we use the integral form in the frequency domain. Because the scattering matrix is defined in the frequency domain, it is convenient to restrict oneself to fields which vary with the time t according to the complex exponential function $e^{\jmath\omega t}$. Then an arbitrary time-depended field $\vec{M}(x,y,z,t)$ can be expressed as

$$\vec{M}(x,y,z,t) = \Re\mathrm{e}(\vec{M}(x,y,z)e^{\jmath\omega t}), \quad \vec{M} \in \{\vec{E},\vec{D},\vec{J},\vec{H},\vec{B}\} \ , \tag{5}$$

where $\vec{M}(x,y,z)$ is the phasor form of $\vec{M}(x,y,z,t)$. $\vec{M}$ is a function of the spatial coordinates only, and in general complex. $\Re\mathrm{e}$ indicates "taking the real part of" quantity in brackets. $\vec{M}$ represents the complex amplitude. Using the phasor representation allows us to replace the time derivations $\frac{\partial}{\partial t}$ by $\jmath\omega$ since

$$\frac{\partial e^{\jmath\omega t}}{\partial t} = \jmath\omega e^{\jmath\omega t} \ . \tag{6}$$

We will not include the factor $e^{\jmath\omega t}$ explicitly as this factor occurs as a common factor in all terms.

$\vec{E}$ $[\frac{V}{m}]$ and $\vec{H}$ $[\frac{A}{m}]$ are the electric and magnetic field intensities, and $\vec{D}$ $[\frac{As}{m^2}]$ and $\vec{B}$ $[\frac{Vs}{m^2}]$ are the electric and magnetic flux densities, respectively. The current density is denoted by $\vec{J}$ $[\frac{A}{m^2}]$. ρ $[\frac{As}{m^3}]$ is the electric charge density. ω $[\frac{1}{s}]$ is the circular frequency of the sinusoidal excitation, and $\jmath^2 = -1$. In the integral form of the first two equations of (4) the surface Ω is an open surface surrounded by a closed contour $\partial\Omega$, while in the last two equations of (4) the surface Ω is a closed surface with an interior volume V. The vector element $\partial\vec{\Omega}$ of area $\partial\Omega$ is directed outward. The direction of the vector element $d\vec{s}$ of the contour $\partial\Omega$ is such that when a right-handed screw is turned in that direction, it will advance in the direction of the vector element $\partial\vec{\Omega}$.

To the Maxwellian equations are added the constitutive relations

$$\vec{B} = \mu\vec{H}, \qquad \vec{D} = \epsilon\vec{E}, \qquad \vec{J} = \kappa\vec{E} + \vec{J}_e \ , \tag{7}$$

describing the macroscopic properties of the medium. In the last equation of (7) the total current density $\vec{J}$ has been split into its conductive part $\kappa\vec{E}$ and its source part $\vec{J}_e$.

In this paper problems of electromagnetic wave propagation are treated. Thus, it is assumed that the field generating charges and currents are located outside of the field domain. That means, the electric charge density ρ and the source current density $\vec{J}_e$ are assumed to be zero in this model:

$$\rho = 0, \quad \vec{J}_e = 0 \ . \tag{8}$$

Then, the last relation of (7) is Ohm's law.

The quantities μ, ϵ, and κ (permeability, permittivity and conductivity) are assumed to be scalar functions of the spatial coordinates.

The quantities μ and ϵ are constant for a vacuum and are denoted by μ_0 $[\frac{Vs}{Am}]$ and ϵ_0 $[\frac{As}{Vm}]$, respectively. In other media μ and ϵ are different from μ_0 and ϵ_0. We write

$$\mu = \mu_r\mu_0, \qquad \epsilon = \epsilon_r\epsilon_0 \ , \tag{9}$$

and call $\mu_r(x,y,z)$ the relative permeability and $\epsilon_r(x,y,z)$ the relative permittivity.

The dimension of κ is $[\frac{1}{\Omega m}]$.
For the sake of simplicity we describe the permittivity ϵ and the conductivity κ by the complex permittivity:

$$\underline{\epsilon} = \epsilon + \frac{\kappa}{\jmath\omega} \ . \tag{10}$$

Similar to (9) we write

$$\mu = \tilde{\mu}\mu_0, \quad \underline{\epsilon} = \tilde{\epsilon}\epsilon_0 \quad \text{with} \quad \tilde{\mu} = \mu_r \ . \tag{11}$$

Taking into account the continuity equation (equation of conservation of electric charge)

$$\nabla \cdot \underline{\vec{J}} = -\frac{\partial \rho}{\partial t} \tag{12}$$

and substituting the constitutive relations (7) into (4) and using (5, 6, 8, 9, 10, 11) the following differential and integral forms of the Maxwellian equations in the frequency domain will result

Differential form			Integral form			
$\nabla \times (\frac{1}{\tilde{\mu}\mu_0}\vec{B})$	$=$	$\jmath\omega\tilde{\epsilon}\epsilon_0\vec{E},$	$\oint_{\partial\Omega} \frac{1}{\tilde{\mu}\mu_0}\vec{B} \cdot d\vec{s}$	$=$	$\int_{\Omega} (\jmath\omega\tilde{\epsilon}\epsilon_0\vec{E}) \cdot d\vec{\Omega},$	
$\nabla \times \vec{E}$	$=$	$-\jmath\omega\vec{B},$	$\oint_{\partial\Omega} \vec{E} \cdot d\vec{s}$	$=$	$\int_{\Omega} (-\jmath\omega\vec{B}) \cdot d\vec{\Omega},$	(13)
$\nabla \cdot (\tilde{\epsilon}\epsilon_0\vec{E})$	$=$	$0,$	$\oint_{\Omega} (\tilde{\epsilon}\epsilon_0\vec{E}) \cdot d\vec{\Omega}$	$=$	$0,$	
$\nabla \cdot \vec{B}$	$=$	$0,$	$\oint_{\Omega} \vec{B} \cdot d\vec{\Omega}$	$=$	$0 \ .$	

Boundary conditions
At the cross-sectional planes p, that is at $z = z_p$, the transverse electric field $\vec{E}_t^{(p)} = \vec{E}_t(z_p)$ is given by superposing transmission line modes $\vec{E}_{t,l}^{(p)} = \vec{E}_{t,l}(z_p)$ with weighted mode-amplitude sums $w_l^{(p)} = w_l(z_p)$:

$$\vec{E}_t^{(p)} = \sum_{l=1}^{m^{(p)}} w_l^{(p)} \vec{E}_{t,l}^{(p)}, \quad p = 1(1)\overline{p}, \quad \vec{E}_t = \sum_{p=1}^{\overline{p}} \vec{E}_t^{(p)} \ . \tag{14}$$

The weighted mode-amplitude sums $w_l^{(p)}$ are given (see [4]).
The transverse electric mode fields $\vec{E}_{t,l}^{(p)}$ are computed using an eigenvalue problem for the transmission lines (see Section 8).
The tangential electric or the tangential magnetic field is assumed to be zero at the rest of the enclosure:

$$\vec{E}_{tang} = 0 \quad \text{or} \quad \vec{H}_{tang} = 0 \ . \tag{15}$$

That is, these parts of the surface are considered to be perfect conductors, either electric or magnetic. The electric case, for example, corresponds with practical applications where the circuits are shielded by a metallic box, whereas magnetic walls correspond to symmetry planes.
At the material boundaries the tangential component of the electric field $\vec{E}_{tang}$, the tangential component of the magnetic field $\vec{H}_{tang}$, the normal component of the electric flux density $\vec{D}_{normal}$ and the normal component of the magnetic flux density $\vec{B}_{normal}$ have to be continuous.

4 The Maxwellian Grid Equations

It is advantageous to solve the Maxwellian equations directly rather than solving a partial differential equation of second order derived therefrom, because the quantities $\tilde{\mu}$ and $\tilde{\epsilon}$ can be different from cell to cell when using Maxwellian equations.
The boundary region is divided into elementary rectangular parallelepipeds (see Figure 2) by using a three-dimensional nonequidistant orthonormal Cartesian grid.
The edges of the cells are parallel to the coordinate axes. The grid nodes (i, j, k), the left corners at the front of the bottom of the parallelepipeds, are numbered by

$$\ell = (k-1)n_x n_y + (j-1)n_x + i, \quad i = 1(1)n_x, \quad j = 1(1)n_y, \quad k = 1(1)n_z. \tag{16}$$

$n_s, s \in \{x, y, z\}$, is the number of rectangular parallelepipeds in the s-direction. Partly we will also characterize the corresponding elementary cells by (i, j, k).
The lengths of the edges which correspond to the grid node (i, j, k) are denoted by $x_{i,j,k}$, $y_{i,j,k}$ and $z_{i,j,k}$.
The field vectors are expressed as

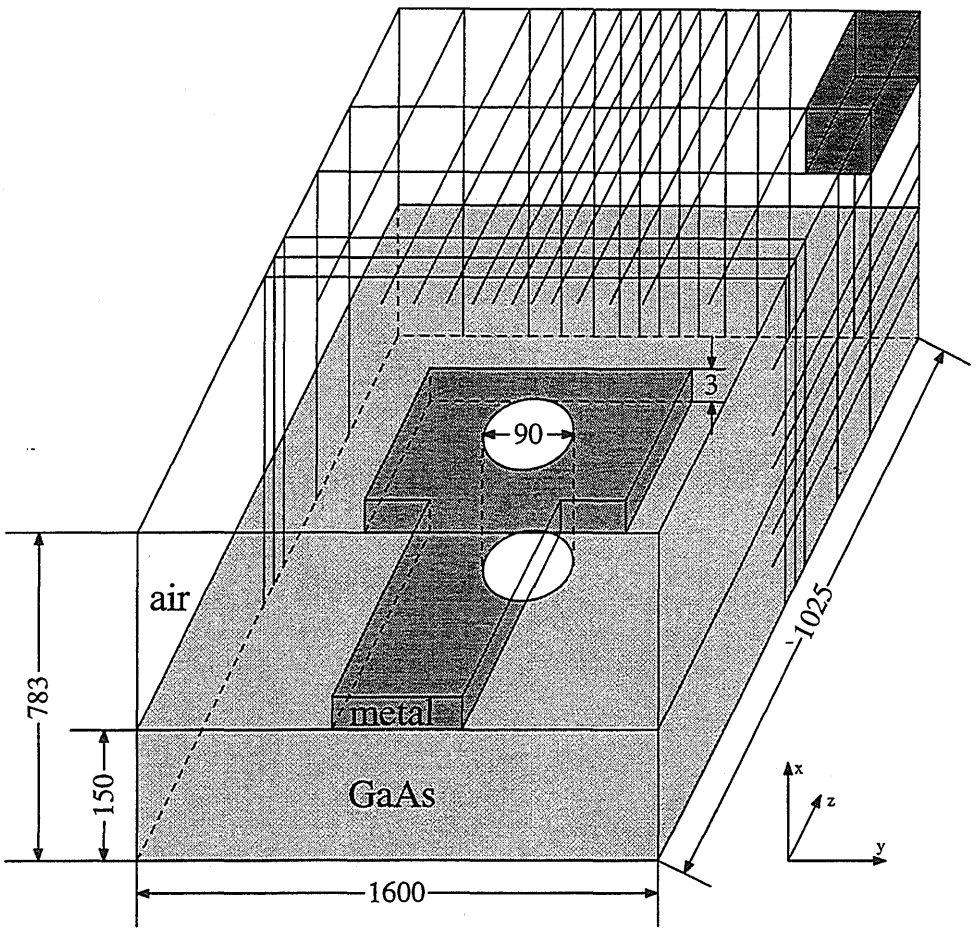

Figure 2: Via hole with a nonequidistant grid of rectangular parallelepipeds (dimensions in μm)

$$\vec{M} = M_x\vec{i}_x + M_y\vec{i}_y + M_z\vec{i}_z, \quad \vec{M} \in \{\vec{E}, \vec{D}, \vec{J}, \vec{H}, \vec{B}\} \ . \tag{17}$$

$\vec{i}_x$, $\vec{i}_y$ and $\vec{i}_z$ are the unit vectors in $x-$, $y-$ and $z-$direction of the Cartesian coordinate grid, respectively. M_x, M_y and M_z are called the x, y and z components of $\vec{M}$. Sometimes we also use the notion component for $M_x\vec{i}_x$, $M_y\vec{i}_y$ and $M_z\vec{i}_z$.
An obvious allocation of the three components of $\vec{E}$ and $\vec{B}$ at the same grid

node is not chosen in order to avoid serious problems at surfaces of materials where some of the field components are not continuous.
Instead of this, the components E_x, E_y and E_z of the electric field $\vec{E}$ are located in the centers of the edges of the elementary cells. The components B_x, B_y and B_z, on the other hand are normal to the face centers [8], [5], [6]. Thus, the electric field components form a primary grid, and the magnetic flux density components a dual grid (see Figure 3).

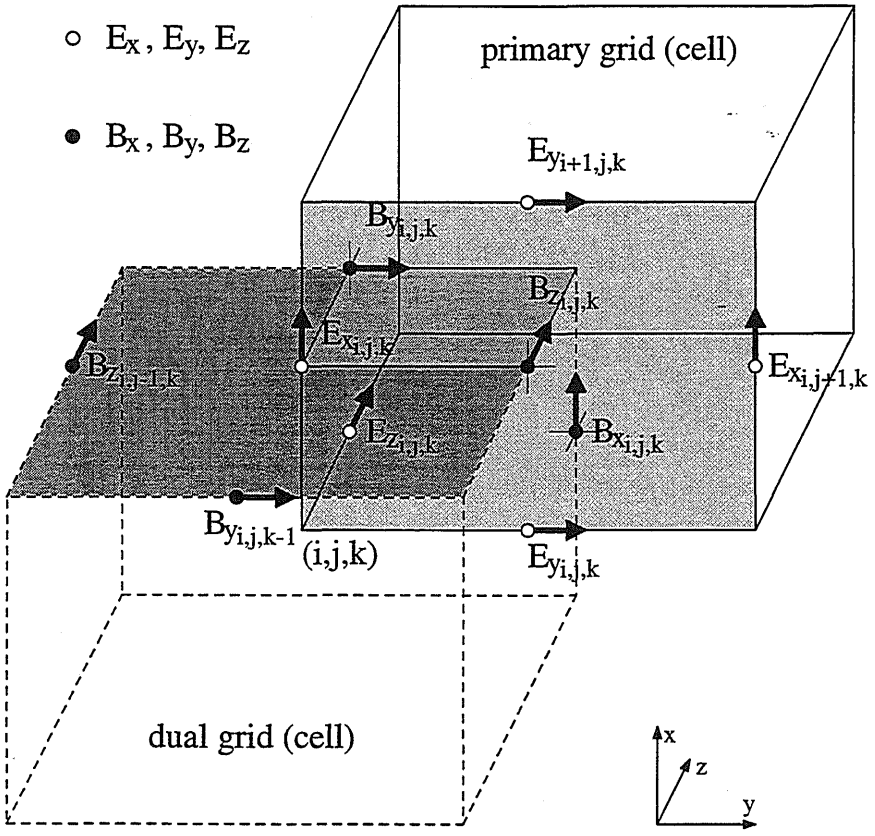

Figure 3: Primary and dual grid

We use the lowest-order integration formulae

$$\oint_{\partial\Omega} \vec{f} \cdot d\vec{s} \approx \sum f_i s_i, \quad \int_{\Omega} \vec{f} \cdot d\vec{\Omega} \approx f\Omega \tag{18}$$

in order to approximate the left-hand and the right-hand sides of the first and the second Maxwellian equation (see (13)).
The closed path $\partial\Omega$ of the integration consists of 4 straight lines of length s_i and is the path around the periphery of an unit cell face in the grid. f_i denotes the function value in the center of the side s_i. The direction of the vectors (see Figure 3) determines the signs of f_i.
Ω is the area of any cell face. f denotes the function value in the center of the surface of this face.

Second Maxwellian equation

If we apply the second Maxwellian equation (see (13)) to the cell faces which correspond to $B_{x_{i,j,k}}$, $B_{y_{i,j,k}}$ and $B_{z_{i,j,k}}$ (see Figure 3, primary grid) using (18) yields

$$y_{i,j,k}E_{y_{i,j,k}} + z_{i,j+1,k}E_{z_{i,j+1,k}} - y_{i,j,k+1}E_{y_{i,j,k+1}} - z_{i,j,k}E_{z_{i,j,k}} = -\jmath\omega y_{i,j,k}z_{i,j,k}B_{x_{i,j,k}} \ , \tag{19}$$

$$z_{i,j,k}E_{z_{i,j,k}} + x_{i,j,k+1}E_{x_{i,j,k+1}} - z_{i+1,j,k}E_{z_{i+1,j,k}} - x_{i,j,k}E_{x_{i,j,k}} = -\jmath\omega x_{i,j,k}z_{i,j,k}B_{y_{i,j,k}} \ , \tag{20}$$

$$x_{i,j,k}E_{x_{i,j,k}} + y_{i+1,j,k}E_{y_{i+1,j,k}} - x_{i,j+1,k}E_{x_{i,j+1,k}} - y_{i,j,k}E_{y_{i,j,k}} = -\jmath\omega x_{i,j,k}y_{i,j,k}B_{z_{i,j,k}} \ . \tag{21}$$

$E_{s_{i,j,k}}$ and $B_{s_{i,j,k}}$, $s \in \{x, y, z\}$, are the function values of the electric field components and of the magnetic flux density components, respectively, in the elementary cell (i, j, k). We do not use half indices.

First Maxwellian equation

Similar equations can be developed for E_x, E_y and E_z if we apply the first Maxwellian equation (see (13)) to the corresponding cell faces (parallel to the (y, z)-, (x, z)- and (x, y)-coordinate plane, respectively) of the dual grid (see Figure 3). Because the material can be different between two elementary cells of the primary grid, we have to divide the integration domain:

$$\frac{1}{2}\left(\frac{z_{i,j,k}}{\tilde{\mu}_{i,j,k}} + \frac{z_{i,j,k-1}}{\tilde{\mu}_{i,j,k-1}}\right)B_{z_{i,j,k}} - \frac{1}{2}\left(\frac{y_{i,j,k}}{\tilde{\mu}_{i,j,k}} + \frac{y_{i,j-1,k}}{\tilde{\mu}_{i,j-1,k}}\right)B_{y_{i,j,k}} -$$
$$\frac{1}{2}\left(\frac{z_{i,j-1,k}}{\tilde{\mu}_{i,j-1,k}} + \frac{z_{i,j-1,k-1}}{\tilde{\mu}_{i,j-1,k-1}}\right)B_{z_{i,j-1,k}} + \frac{1}{2}\left(\frac{y_{i,j-1,k-1}}{\tilde{\mu}_{i,j-1,k-1}} + \frac{y_{i,j,k-1}}{\tilde{\mu}_{i,j,k-1}}\right)B_{y_{i,j,k-1}}$$
$$= \jmath\omega\epsilon_0\mu_0 g^{y,z}_{i,j,k}E_{x_{i,j,k}} \ , \tag{22}$$

$$\frac{1}{2}\left(\frac{x_{i,j,k}}{\tilde{\mu}_{i,j,k}}+\frac{x_{i-1,j,k}}{\tilde{\mu}_{i-1,j,k}}\right)B_{x_{i,j,k}}-\frac{1}{2}\left(\frac{z_{i,j,k}}{\tilde{\mu}_{i,j,k}}+\frac{z_{i,j,k-1}}{\tilde{\mu}_{i,j,k-1}}\right)B_{z_{i,j,k}}-$$

$$\frac{1}{2}\left(\frac{x_{i,j,k-1}}{\tilde{\mu}_{i,j,k-1}}+\frac{x_{i-1,j,k-1}}{\tilde{\mu}_{i-1,j,k-1}}\right)B_{x_{i,j,k-1}}+\frac{1}{2}\left(\frac{z_{i-1,j,k-1}}{\tilde{\mu}_{i-1,j,k-1}}+\frac{z_{i-1,j,k}}{\tilde{\mu}_{i-1,j,k}}\right)B_{z_{i-1,j,k}}$$

$$= \jmath\omega\epsilon_0\mu_0 g^{x,z}_{i,j,k}E_{y_{i,j,k}} \ , \tag{23}$$

$$\frac{1}{2}\left(\frac{y_{i,j,k}}{\tilde{\mu}_{i,j,k}}+\frac{y_{i,j-1,k}}{\tilde{\mu}_{i,j-1,k}}\right)B_{y_{i,j,k}}-\frac{1}{2}\left(\frac{x_{i,j,k}}{\tilde{\mu}_{i,j,k}}+\frac{x_{i-1,j,k}}{\tilde{\mu}_{i-1,j,k}}\right)B_{x_{i,j,k}}-$$

$$\frac{1}{2}\left(\frac{y_{i-1,j,k}}{\tilde{\mu}_{i-1,j,k}}+\frac{y_{i-1,j-1,k}}{\tilde{\mu}_{i-1,j-1,k}}\right)B_{y_{i-1,j,k}}+\frac{1}{2}\left(\frac{x_{i-1,j-1,k}}{\tilde{\mu}_{i-1,j-1,k}}+\frac{x_{i,j-1,k}}{\tilde{\mu}_{i,j-1,k}}\right)B_{x_{i,j-1,k}}$$

$$= \jmath\omega\epsilon_0\mu_0 g^{x,y}_{i,j,k}E_{z_{i,j,k}} \ . \tag{24}$$

The $g^{y,z}$, $g^{x,z}$ and $g^{x,y}$ are declared in (26), (27) and (28), respectively.
The Equations (19 - 24) form a system of linear algebraic equations for the computation of the electromagnetic field in the absence of any boundary conditions.

Electric-field divergence

Dividing the integration domain of the dual grid in order to take into account the different material of the elementary cells and discretizing the third equation in (13) (see Figure 3) yields

$$g^{y,z}_{i,j,k}E_{x_{i,j,k}}-g^{y,z}_{i-1,j,k}E_{x_{i-1,j,k}}+g^{x,z}_{i,j,k}E_{y_{i,j,k}}-g^{x,z}_{i,j-1,k}E_{y_{i,j-1,k}}+$$

$$g^{x,y}_{i,j,k}E_{z_{i,j,k}}-g^{x,y}_{i,j,k-1}E_{z_{i,j,k-1}}=0 \tag{25}$$

with

$$g^{y,z}_{i,j,k}=\left(\frac{y_{i,j,k}z_{i,j,k}}{4}\tilde{\epsilon}_{i,j,k}+\frac{y_{i,j-1,k}z_{i,j-1,k}}{4}\tilde{\epsilon}_{i,j-1,k}+\right.$$

$$\left.\frac{y_{i,j-1,k-1}z_{i,j-1,k-1}}{4}\tilde{\epsilon}_{i,j-1,k-1}+\frac{y_{i,j,k-1}z_{i,j,k-1}}{4}\tilde{\epsilon}_{i,j,k-1}\right) \ , \tag{26}$$

$$g^{x,z}_{i,j,k}=\left(\frac{x_{i,j,k}z_{i,j,k}}{4}\tilde{\epsilon}_{i,j,k}+\frac{x_{i,j,k-1}z_{i,j,k-1}}{4}\tilde{\epsilon}_{i,j,k-1}+\right.$$

$$\left.\frac{x_{i-1,j,k-1}z_{i-1,j,k-1}}{4}\tilde{\epsilon}_{i-1,j,k-1}+\frac{x_{i-1,j,k}z_{i-1,j,k}}{4}\tilde{\epsilon}_{i-1,j,k}\right) \ , \tag{27}$$

$$g^{x,y}_{i,j,k} = (\frac{x_{i,j,k}y_{i,j,k}}{4}\tilde{\epsilon}_{i,j,k} + \frac{x_{i-1,j,k}y_{i-1,j,k}}{4}\tilde{\epsilon}_{i-1,j,k} +$$

$$\frac{x_{i-1,j-1,k}y_{i-1,j-1,k}}{4}\tilde{\epsilon}_{i-1,j-1,k} + \frac{x_{i,j-1,k}y_{i,j-1,k}}{4}\tilde{\epsilon}_{i,j-1,k}) \ . \qquad (28)$$

Magnetic-field divergence

The primary grid is used to discretize the forth equation of (13):

$$y_{i,j,k}z_{i,j,k}B_{x_{i,j,k}} - y_{i+1,j,k}z_{i+1,j,k}B_{x_{i+1,j,k}} +$$

$$x_{i,j,k}z_{i,j,k}B_{y_{i,j,k}} - x_{i,j+1,k}z_{i,j+1,k}B_{y_{i,j+1,k}} +$$

$$x_{i,j,k}y_{i,j,k}B_{z_{i,j,k}} - x_{i,j,k+1}y_{i,j,k+1}B_{z_{i,j,k+1}} = 0 \ . \qquad (29)$$

Remark

We note that using the differential form of the Maxwellian equations the grid equations (19) - (24), (25) and (29) also may be derived by the finite-difference method [8] instead of the above used finite-volume method.

5 The System of Linear Algebraic Equations

The number of unknowns in the system of linear algebraic Equations (19 - 24) can be reduced by a factor of two. Substituting the components of the magnetic flux density in (22 - 24) using (19 - 21) and using corresponding manipulations of the second Maxwellian equation to neighboring elementary cells yields

$$c^{z,x}_{i,j,k}E_{y_{i+1,j,k}} - c^{z,y}_{i,j,k}E_{x_{i,j+1,k}} - c^{z,x}_{i,j,k}E_{y_{i,j,k}} - c^{y,x}_{i,j,k}E_{z_{i,j,k}} -$$

$$c^{y,z}_{i,j,k}E_{x_{i,j,k+1}} + c^{y,x}_{i,j,k}E_{z_{i+1,j,k}} - c^{z,y}_{i,j-1,k}E_{x_{i,j-1,k}} - c^{z,x}_{i,j-1,k}E_{y_{i+1,j-1,k}} +$$

$$c^{z,x}_{i,j-1,k}E_{y_{i,j-1,k}} + c^{y,x}_{i,j,k-1}E_{z_{i,j,k-1}} - c^{y,x}_{i,j,k-1}E_{z_{i+1,j,k-1}} - c^{y,z}_{i,j,k-1}E_{x_{i,j,k-1}} +$$

$$(c^{z,y}_{i,j,k} + c^{y,z}_{i,j,k} + c^{z,y}_{i,j-1,k} + c^{y,z}_{i,j,k-1} - 2\varkappa_0^2 g^{y,z}_{i,j,k})E_{x_{i,j,k}} = 0 \ , \qquad (30)$$

$$
\begin{aligned}
&c^{x,y}_{i,j,k}E_{z_{i,j+1,k}} - c^{x,z}_{i,j,k}E_{y_{i,j,k+1}} - c^{x,y}_{i,j,k}E_{z_{i,j,k}} - c^{z,y}_{i,j,k}E_{x_{i,j,k}} - \\
&c^{z,x}_{i,j,k}E_{y_{i+1,j,k}} + c^{z,y}_{i,j,k}E_{x_{i,j+1,k}} - c^{x,z}_{i,j,k-1}E_{y_{i,j,k-1}} - c^{x,y}_{i,j,k-1}E_{z_{i,j+1,k-1}} + \\
&c^{x,y}_{i,j,k-1}E_{z_{i,j,k-1}} + c^{z,y}_{i-1,j,k}E_{x_{i-1,j,k}} - c^{z,y}_{i-1,j,k}E_{x_{i-1,j+1,k}} - c^{z,x}_{i-1,j,k}E_{y_{i-1,j,k}} + \\
&\qquad (c^{x,z}_{i,j,k} + c^{z,x}_{i,j,k} + c^{x,z}_{i,j,k-1} + c^{z,x}_{i-1,j,k} - 2\varkappa_0^2 g^{x,z}_{i,j,k})E_{y_{i,j,k}} = 0 \ , \qquad (31)
\end{aligned}
$$

$$
\begin{aligned}
&c^{y,z}_{i,j,k}E_{x_{i,j,k+1}} - c^{y,x}_{i,j,k}E_{z_{i+1,j,k}} - c^{y,z}_{i,j,k}E_{x_{i,j,k}} - c^{x,z}_{i,j,k}E_{y_{i,j,k}} - \\
&c^{x,y}_{i,j,k}E_{z_{i,j+1,k}} + c^{x,z}_{i,j,k}E_{y_{i,j,k+1}} - c^{y,x}_{i-1,j,k}E_{z_{i-1,j,k}} - c^{y,z}_{i-1,j,k}E_{x_{i-1,j,k+1}} + \\
&c^{y,z}_{i-1;j,k}E_{x_{i-1,j,k}} + c^{x,z}_{i,j-1,k}E_{y_{i,j-1,k}} - c^{x,z}_{i,j-1,k}E_{y_{i,j-1,k+1}} - c^{x,y}_{i,j-1,k}E_{z_{i,j-1,k}} + \\
&\qquad (c^{y,x}_{i,j,k} + c^{x,y}_{i,j,k} + c^{y,x}_{i-1,j,k} + c^{x,y}_{i,j-1,k} - 2\varkappa_0^2 g^{x,y}_{i,j,k})E_{z_{i,j,k}} = 0 \qquad (32)
\end{aligned}
$$

with

$$
\varkappa_0 = \omega\sqrt{\epsilon_0\mu_0} \ , \qquad (33)
$$

$$
c^{s,t}_{i,j,k} = \left(\frac{s_{i,j,k}}{\tilde{\mu}_{i,j,k}} + \frac{s_{i',j',k'}}{\tilde{\mu}_{i',j',k'}}\right)\frac{1}{t_{i,j,k}} \quad , \quad s,t \in \{x,y,z\} \ . \qquad (34)
$$

(i',j',k') are the indices of the elementary cell which is located in s-direction in front of the cell (i,j,k):

$$
\begin{aligned}
s = x: &\quad i' = i-1, \quad j' = j, \quad k' = k \ , \\
s = y: &\quad i' = i, \quad j' = j-1, \quad k' = k \ , \\
s = z: &\quad i' = i, \quad j' = j, \quad k' = k-1 \ .
\end{aligned}
$$

Because we use a Cartesian grid, we have

$$
\begin{aligned}
x_{i,j,k} &= x_{i,j-1,k} = x_{i,j+1,k} = x_{i,j,k-1} = x_{i,j,k+1} \ , \\
y_{i,j,k} &= y_{i+1,j,k} = y_{i-1,j,k} = y_{i,j,k-1} = y_{i,j,k+1} \ , \\
z_{i,j,k} &= z_{i+1,j,k} = z_{i-1,j,k} = z_{i,j-1,k} = z_{i,j+1,k} \ , \\
x_{i-1,j,k} &= x_{i-1,j-1,k} = x_{i-1,j,k-1} \ , \\
y_{i,j-1,k} &= y_{i-1,j-1,k} = y_{i,j-1,k-1} \ , \\
z_{i,j,k-1} &= z_{i-1,j,k-1} = z_{i,j-1,k-1} \ .
\end{aligned} \qquad (35)
$$

$\varkappa_0$ is the wavenumber in vacuo.

6 The Matrix Representation of the Maxwellian Equations

Second Maxwellian equation

Let be

$$\begin{aligned}
\vec{e} = (\vec{e}_x, \vec{e}_y, \vec{e}_z)^T \quad , \quad \vec{e}_x &= (e_{x_1}, e_{x_2}, \ldots, e_{x_{n_{xyz}}}) \quad , \quad e_{x_\ell} = E_{x_{i,j,k}} \quad , \\
\vec{e}_y &= (e_{y_1}, e_{y_2}, \ldots, e_{y_{n_{xyz}}}) \quad , \quad e_{y_\ell} = E_{y_{i,j,k}} \quad , \\
\vec{e}_z &= (e_{z_1}, e_{z_2}, \ldots, e_{z_{n_{xyz}}}) \quad , \quad e_{z_\ell} = E_{z_{i,j,k}} \quad , \\
\vec{b} = (\vec{b}_x, \vec{b}_y, \vec{b}_z)^T \quad , \quad \vec{b}_x &= (b_{x_1}, b_{x_2}, \ldots, b_{x_{n_{xyz}}}) \quad , \quad b_{x_\ell} = B_{x_{i,j,k}} \quad , \\
\vec{b}_y &= (b_{y_1}, b_{y_2}, \ldots, b_{y_{n_{xyz}}}) \quad , \quad b_{y_\ell} = B_{y_{i,j,k}} \quad , \\
\vec{b}_z &= (b_{z_1}, b_{z_2}, \ldots, b_{z_{n_{xyz}}}) \quad , \quad b_{z_\ell} = B_{z_{i,j,k}}
\end{aligned} \tag{36}$$

with

$$\ell = (k-1)n_{xy} + (j-1)n_x + i, \quad n_{xy} = n_x n_y, \quad n_{xyz} = n_x n_y n_z \quad , \tag{37}$$

the vectors containing the electric and the magnetic field of the elementary cells, respectively, in the system of the linear algebraic Equations (19 - 24). Let be

$$\begin{aligned}
D_s \;=\; diag(\; & \cdots, x_{i,j,k}, x_{i+1,j,k}, \cdots, x_{i,j+1,k}, \cdots, x_{i,j,k+1}, \\
& \cdots, y_{i,j,k}, y_{i+1,j,k}, \cdots, y_{i,j+1,k}, \cdots, y_{i,j,k+1}, \\
& \cdots, z_{i,j,k}, z_{i+1,j,k}, \cdots, z_{i,j+1,k}, \cdots, z_{i,j,k+1}, \cdots \;) \quad ,
\end{aligned} \tag{38}$$

$$D_A \;=\; diag(\; \cdots, y_{i,j,k}z_{i,j,k}, \cdots, x_{i,j,k}z_{i,j,k}, \cdots, x_{i,j,k}y_{i,j,k}, \cdots \;) \tag{39}$$

diagonal matrices and A the following matrix:

$$A = \tag{40}$$

positon	$E_{x_{i,j,k}}$	$E_{x_{i+1,j,k}}$	$E_{x_{i,j+1,k}}$	$E_{x_{i,j,k+1}}$	$E_{y_{i,j,k}}$	$E_{y_{i+1,j,k}}$	$E_{y_{i,j+1,k}}$	$E_{y_{i,j,k+1}}$	$E_{z_{i,j,k}}$	$E_{z_{i+1,j,k}}$	$E_{z_{i,j+1,k}}$	$E_{z_{i,j,k+1}}$
ℓ	**0**	0	0	0	1	0	0	−1	−1	0	1	0
$n_{xyz}+\ell-n_{xy}$	1	0	0	0	0	0	0	0	0	0	0	0
$n_{xyz}+\ell$	−1	0	0	1	**0**	0	0	0	1	−1	0	0
$2n_{xyz}+\ell-n_x$	−1	0	0	0	0	0	0	0	0	0	0	0
$2n_{xyz}+\ell$	1	0	−1	0	−1	1	0	0	**0**	0	0	0

The elements of A contained in a box are diagonal elements.
The following scheme gives distances between the columns which contain the diagonal element and the values 1 and -1 in the first row of A. For example, n_{xy} is the distance between the columns which correspond to $E_{y_{i,j,k}}$ and $E_{y_{i,j,k+1}}$.

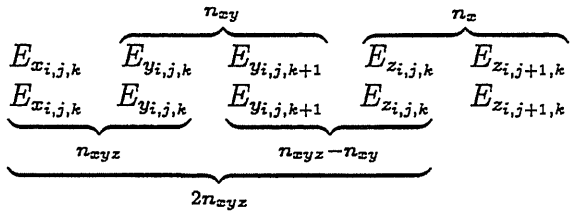

A is defined as the operator of the line integral and represents the curl operator in the second Maxwellian equation (see (13)) using the primary grid. The diagonal matrices D_s and D_A contain the information on dimension for the structure and the corresponding mesh. The represented rows of A correspond to the left-hand side of the Equations (19), (20) and (21) in this order extracting D_s. Using the denotations (36), (37), (38), (39) and the definition of A the following matrix representation of the second Maxwellian equation results from (19) - (21):

$$\oint_{\partial\Omega} \vec{E} \cdot d\vec{s} = \int_{\Omega} (-\jmath\omega\vec{B}) \cdot d\vec{\Omega} \quad \Rightarrow \quad AD_s\vec{e} = -\jmath\omega D_A\vec{b} \ . \tag{41}$$

First Maxwellian equation

Let be

$$\begin{aligned} D_{s/\tilde{\mu}} \ = \ & diag(\cdots, \tfrac{1}{2}(\tfrac{x_{i,j,k-1}}{\tilde{\mu}_{i,j,k-1}} + \tfrac{x_{i-1,j,k-1}}{\tilde{\mu}_{i-1,j,k-1}}), \cdots, \tfrac{1}{2}(\tfrac{x_{i-1,j-1,k}}{\tilde{\mu}_{i-1,j-1,k}} + \tfrac{x_{i,j-1,k}}{\tilde{\mu}_{i,j-1,k}}), \\ & \cdots, \tfrac{1}{2}(\tfrac{x_{i-1,j,k}}{\tilde{\mu}_{i-1,j,k}} + \tfrac{x_{i-2,j,k}}{\tilde{\mu}_{i-2,j,k}}), \tfrac{1}{2}(\tfrac{x_{i,j,k}}{\tilde{\mu}_{i,j,k}} + \tfrac{x_{i-1,j,k}}{\tilde{\mu}_{i-1,j,k}}), \\ & \cdots, \tfrac{1}{2}(\tfrac{y_{i,j-1,k-1}}{\tilde{\mu}_{i,j-1,k-1}} + \tfrac{y_{i,j,k-1}}{\tilde{\mu}_{i,j,k-1}}), \cdots, \tfrac{1}{2}(\tfrac{y_{i,j-1,k}}{\tilde{\mu}_{i,j-1,k}} + \tfrac{y_{i,j-2,k}}{\tilde{\mu}_{i,j-2,k}}), \\ & \cdots, \tfrac{1}{2}(\tfrac{y_{i-1,j,k}}{\tilde{\mu}_{i-1,j,k}} + \tfrac{y_{i-1,j-1,k}}{\tilde{\mu}_{i-1,j-1,k}}), \tfrac{1}{2}(\tfrac{y_{i,j,k}}{\tilde{\mu}_{i,j,k}} + \tfrac{y_{i,j-1,k}}{\tilde{\mu}_{i,j-1,k}}), \\ & \cdots, \tfrac{1}{2}(\tfrac{z_{i,j,k-1}}{\tilde{\mu}_{i,j,k-1}} + \tfrac{z_{i,j,k-2}}{\tilde{\mu}_{i,j,k-2}}), \cdots, \tfrac{1}{2}(\tfrac{z_{i,j-1,k}}{\tilde{\mu}_{i,j-1,k}} + \tfrac{z_{i,j-1,k-1}}{\tilde{\mu}_{i,j-1,k-1}}), \\ & \cdots, \tfrac{1}{2}(\tfrac{z_{i-1,j,k-1}}{\tilde{\mu}_{i-1,j,k-1}} + \tfrac{z_{i-1,j,k}}{\tilde{\mu}_{i-1,j,k}}), \tfrac{1}{2}(\tfrac{z_{i,j,k}}{\tilde{\mu}_{i,j,k}} + \tfrac{z_{i,j,k-1}}{\tilde{\mu}_{i,j,k-1}}), \cdots) \ , \end{aligned} \tag{42}$$

$$D_{A_{\tilde{\epsilon}}} = diag(\ \cdots, g^{y,z}_{i,j,k}, \cdots, g^{x,z}_{i,j,k}, \cdots, g^{x,y}_{i,j,k}, \cdots \ ) \tag{43}$$

diagonal matrices and $\bar{A}$ the following matrix:

$$\bar{A} = \tag{44}$$

position	$B_{x_{i,j,k-1}}$	$B_{x_{i,j-1,k}}$	$B_{x_{i-1,j,k}}$	$B_{x_{i,j,k}}$	$B_{y_{i,j,k-1}}$	$B_{y_{i,j-1,k}}$	$B_{y_{i-1,j,k}}$	$B_{y_{i,j,k}}$	$B_{z_{i,j,k-1}}$	$B_{z_{i,j-1,k}}$	$B_{z_{i-1,j,k}}$	$B_{z_{i,j,k}}$
ℓ	0	0	0	**0**	1	0	0	−1	0	−1	0	1
$n_{xyz}+\ell$	−1	0	0	1	0	0	0	**0**	0	0	1	−1
$n_{xyz}+\ell+n_{xy}$	0	0	0	−1	0	0	0	0	0	0	0	0
$2n_{xyz}+\ell$	0	1	0	−1	0	0	−1	1	0	0	0	**0**
$2n_{xyz}+\ell+n_x$	0	0	0	1	0	0	0	0	0	0	0	0

The elements of $\bar{A}$ contained in a box are diagonal elements.
The following scheme gives distances between the columns which contain the diagonal element and the values 1 and -1 in the first row of $\bar{A}$. For example, n_{xy} is the distance between the columns which correspond to $B_{y_{i,j,k-1}}$ and $B_{y_{i,j,k}}$.

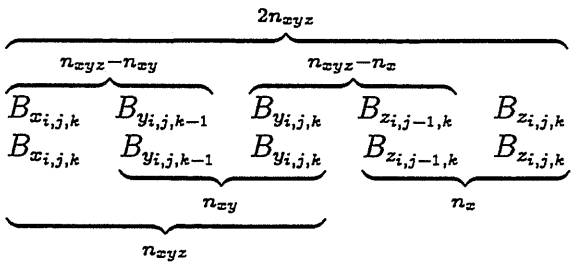

$\bar{A}$ is defined as the operator of the line integral and represents the curl operator in the first Maxwellian equation (see (13)) using the dual grid.
The diagonal matrices $D_{s/\tilde{\mu}}$ and $D_{A_{\tilde{\epsilon}}}$ contain the information on dimension and material for the structure and the corresponding mesh. The represented rows of $\bar{A}$ correspond to the left-hand side of the Equations (22), (23) and (24) in this order extracting $D_{s/\tilde{\mu}}$.
Because of $\bar{A} = A^T$ we get with the denotations (36), (37), (42) and (43) the following matrix representation of the first Maxwellian equation from (22) - (24):

$$\oint_{\partial\Omega} \frac{\vec{B}}{\tilde{\mu}} \cdot d\vec{s} = \int_{\Omega} (\jmath\omega\tilde{\epsilon}\epsilon_0\mu_0\vec{E}) \cdot d\vec{\Omega} \quad \Rightarrow \quad A^T D_{s/\tilde{\mu}} \vec{b} = \jmath\omega\epsilon_0\mu_0 D_{A\tilde{\epsilon}}\vec{e} \ . \tag{45}$$

The system of linear algebraic equations
Using (33) we get from (41) and (45) the matrix representation of the system of linear algebraic Equations (30) - (32):

$$Q_1\vec{e} = 0, \quad Q_1 = A^T D_{s/\tilde{\mu}} D_A^{-1} A D_s - \varkappa_0^2 D_{A\tilde{\epsilon}} \tag{46}$$

with (see (34))

$$Q_1 = (c_{i,j,k}^{s,t}) \ .$$

We have to take into account the boundary conditions (14, 15) in (46). Thus, we get from (46) a partitioning of the matrix Q_1 into the sum of two matrices:

$$Q_1\vec{e} = (Q_{1,A} + Q_{1,r})\vec{e} = 0 \ , \tag{47}$$

where $Q_{1,r}\vec{e}$ is known.
The matrix $Q_{1,r}$ contains coefficients of the corresponding rows and columns of the matrix Q_1. The matrix Q_1 of (47) is transformed into a symmetric one, after some mathematical manipulations:

$$\begin{aligned} \tilde{Q}_1\tilde{\vec{e}} &= D_s^{\frac{1}{2}} Q_1 D_s^{-\frac{1}{2}} D_s^{\frac{1}{2}} \vec{e} \\ &= (D_s^{\frac{1}{2}} Q_{1,A} D_s^{-\frac{1}{2}} + D_s^{\frac{1}{2}} Q_{1,r} D_s^{-\frac{1}{2}}) D_s^{\frac{1}{2}} \vec{e} \\ &= (\tilde{Q}_{1,A} + \tilde{Q}_{1,r})\tilde{\vec{e}} \\ &= 0 \end{aligned} \tag{48}$$

with

$$\tilde{Q}_{1,A} = D_s^{\frac{1}{2}} Q_{1,A} D_s^{-\frac{1}{2}} \ , \ \tilde{Q}_{1,r} = D_s^{\frac{1}{2}} Q_{1,r} D_s^{-\frac{1}{2}} \ , \ \vec{\tilde{e}} = D_s^{\frac{1}{2}} \vec{e} \ , \tag{49}$$

and

$$\tilde{Q}_1 = D_s^{\frac{1}{2}} A^T D_{s/\tilde{\mu}} D_A^{-1} A D_s^{\frac{1}{2}} - \varkappa_0^2 D_{A\tilde{\varepsilon}} \ . \tag{50}$$

The matrix $\tilde{Q}_1$ from (48, 49, 50) is obviously a symmetric matrix. $\tilde{Q}_{1,r}$ depends on the position of the cross-sectional planes p and is also a symmetric matrix (see example in this section and Figure 5). Thus, $\tilde{Q}_{1,A}$ is also a symmetric matrix because of $(\tilde{Q}_{1,A})^T = (\tilde{Q}_1 - \tilde{Q}_{1,r})^T = \tilde{Q}_1 - \tilde{Q}_{1,r} = \tilde{Q}_{1,A}$.
We get from (48) the system of linear algebraic equations with the matrix $\tilde{Q}_{1,A}$:

$$\tilde{Q}_{1,A} \vec{\tilde{e}} = -\tilde{Q}_{1,r} \vec{\tilde{e}} = -D_s^{\frac{1}{2}} Q_{1,r} D_s^{-\frac{1}{2}} D_s^{\frac{1}{2}} \vec{e} = \vec{\tilde{r}} \tag{51}$$

with

$$\vec{\tilde{r}} = D_s^{\frac{1}{2}} \vec{r} \quad , \quad \vec{r} = -Q_{1,r} \vec{e} \ , \tag{52}$$

and

$$\begin{aligned} \vec{r} = (\vec{r}_x, \vec{r}_y, \vec{r}_z)^T \ , \quad \vec{r}_x &= (r_{x_1}, r_{x_2}, \ldots, r_{x_{n_{xyz}}}) \ , \\ \vec{r}_y &= (r_{y_1}, r_{y_2}, \ldots, r_{y_{n_{xyz}}}) \ , \\ \vec{r}_z &= (r_{z_1}, r_{z_2}, \ldots, r_{z_{n_{xyz}}}) \ . \end{aligned} \tag{53}$$

We do not solve the system of linear algebraic equations in this form, but we add the gradient of the third Maxwellian equation (see (13)) to (51). A motivation for this is given in [4].

The electric-field divergence and
the modified system of linear algebraic equations
Extracting $D_{A\tilde{\varepsilon}}$ the matrix B (see (54)) results from (25). B consists of 3 submatrices because of homogeneity with the first Maxwellian equation. The submatrix of B is defined as the operator of the surface integral or of the divergence in the 3rd equation of (13) using the dual grid.
The elements of B contained in a box are diagonal elements.

$$B = \tag{54}$$

position	$E_{x_{i-1,j,k}}$	$E_{x_{i,j,k}}$	$E_{x_{i+1,j,k}}$	$E_{y_{i,j-1,k}}$	$E_{y_{i+1,j-1,k}}$	$E_{y_{i,j,k}}$	$E_{y_{i+1,j,k}}$	$E_{z_{i,j,k-1}}$	$E_{z_{i+1,j,k-1}}$	$E_{z_{i,j,k}}$	$E_{z_{i+1,j,k}}$
$\ell+1$ ℓ	-1	$\boxed{1}$		-1		1		-1		1	
		-1	$\boxed{1}$		-1		1		-1		1
$n_{wyz}+\ell$	-1	1		-1		$\boxed{1}$		-1		1	
$n_{xyz}+\ell+n_w$		-1	1		-1		1		-1		1
$2n_{wyz}+\ell$	-1	1		-1		1		-1		$\boxed{1}$	
$2n_{wyz}+\ell+n_{wy}$		-1	1		-1		1		-1		1

The following scheme gives distances between the columns which contain the diagonal element and the values 1 and -1 in the first row of B. For example,

n_x is the distance between the columns which correspond to $E_{y_{i,j-1,k}}$ and $E_{y_{i,j,k}}$.

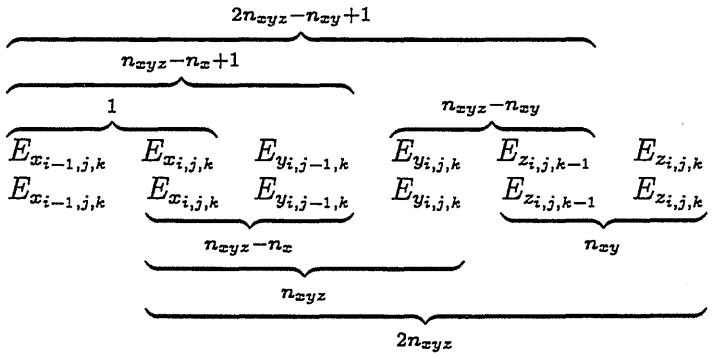

With (43) and the definition of B we get the following matrix representation of the third equation of (13):

$$\oint_{\Omega} \tilde{\epsilon}\epsilon_0 \vec{E} \cdot d\vec{\Omega} = 0 \quad \Rightarrow \quad BD_{A\tilde{\epsilon}}\vec{e} = 0 \ . \tag{55}$$

Equation (55) can be written without loosing generality as

$$Q_2\vec{e} = 0 \quad \text{with} \quad Q_2 = D_s^{-1} D_{A\tilde{\epsilon}} B^T D_{V\tilde{\epsilon}\tilde{\epsilon}}^{-1} B D_{A\tilde{\epsilon}} \ . \tag{56}$$

with

$$D_{V\tilde{\epsilon}\tilde{\epsilon}} = diag(\cdots, d_{V\tilde{\epsilon}\tilde{\epsilon}_{i,j,k}}, d_{V\tilde{\epsilon}\tilde{\epsilon}_{i,j,k}}, d_{V\tilde{\epsilon}\tilde{\epsilon}_{i,j,k}}, \cdots) \tag{57}$$

with

$$\begin{aligned} d_{V\tilde{\epsilon}\tilde{\epsilon}_{i,j,k}} \ = \ & \tfrac{1}{8}(x_{i-1,j-1,k-1}y_{i-1,j-1,k-1}z_{i-1,j-1,k-1}\tilde{\epsilon}^2_{i-1,j-1,k-1} + \\ & x_{i,j-1,k-1}y_{i,j-1,k-1}z_{i,j-1,k-1}\tilde{\epsilon}^2_{i,j-1,k-1} + \\ & x_{i-1,j,k-1}y_{i-1,j,k-1}z_{i-1,j,k-1}\tilde{\epsilon}^2_{i-1,j,k-1} + \\ & x_{i,j,k-1}y_{i,j,k-1}z_{i,j,k-1}\tilde{\epsilon}^2_{i,j,k-1} + \\ & x_{i-1,j-1,k}y_{i-1,j-1,k}z_{i-1,j-1,k}\tilde{\epsilon}^2_{i-1,j-1,k} + \\ & x_{i,j-1,k}y_{i,j-1,k}z_{i,j-1,k}\tilde{\epsilon}^2_{i,j-1,k} + \\ & x_{i-1,j,k}y_{i-1,j,k}z_{i-1,j,k}\tilde{\epsilon}^2_{i-1,j,k} + x_{i,j,k}y_{i,j,k}z_{i,j,k}\tilde{\epsilon}^2_{i,j,k}) \ . \end{aligned} \tag{58}$$

Equation (56) is equivalent to (see [4])

$$\nabla(\nabla \cdot \tilde{\epsilon}\epsilon_0 \vec{E}) = 0 \ . \tag{59}$$

We can transform Equation (56) into

$$\tilde{Q}_2\vec{\tilde{e}} = 0 \quad \text{with} \quad \tilde{Q}_2 = D_s^{\frac{1}{2}} Q_2 D_s^{-\frac{1}{2}}, \quad \vec{\tilde{e}} = D_s^{\frac{1}{2}}\vec{e} \ . \tag{60}$$

$\tilde{Q}_2$ is obviously a symmetric matrix. The matrix $\tilde{Q}_2$ will be connected together with $\tilde{Q}_{1,A}$. Therefore, we carry out a similar partitioning like (48). We get from(60):

$$\tilde{Q}_2\vec{\tilde{e}} = (\tilde{Q}_{2,A} + \tilde{Q}_{2,r})\vec{\tilde{e}} = 0 \tag{61}$$

with

$$\tilde{Q}_{2,r}\vec{\tilde{e}} = 0 \ . \tag{62}$$

$\tilde{Q}_{2,r}$ depends on the position of the cross-sectional planes p and is a symmetric matrix (see example in this section and Figure 6). Thus, $\tilde{Q}_{2,A}$ is also a symmetric matrix because of $(\tilde{Q}_{2,A})^T = (\tilde{Q}_2 - \tilde{Q}_{2,r})^T = \tilde{Q}_2 - \tilde{Q}_{2,r} = \tilde{Q}_{2,A}$. We get the system of linear algebraic equations with the matrix $\tilde{Q}_{2,A}$:

$$\tilde{Q}_{2,A}\vec{\tilde{e}} = 0 \ . \tag{63}$$

We add the Equation (63) to Equation (51) with (52).
Thus, we get

$$\tilde{Q}_A\vec{\tilde{e}} = (\tilde{Q}_{1,A} + \tilde{Q}_{2,A})\vec{\tilde{e}} = \vec{\tilde{r}} \tag{64}$$

with

$$\tilde{Q} = \tilde{Q}_A + \tilde{Q}_r \ , \ \tilde{Q}_A = \tilde{Q}_{1,A} + \tilde{Q}_{2,A} \ , \ \tilde{Q}_r = \tilde{Q}_{1,r} + \tilde{Q}_{2,r} \ , \tag{65}$$

and

$$\begin{aligned} \tilde{Q} &= \tilde{Q}_{1,A} + \tilde{Q}_{1,r} + \tilde{Q}_{2,A} + \tilde{Q}_{2,r} \\ &= \tilde{Q}_1 + \tilde{Q}_2 \\ &= D_s^{\frac{1}{2}} Q_1 D_s^{-\frac{1}{2}} + D_s^{\frac{1}{2}} Q_2 D_s^{-\frac{1}{2}} \\ &= D_s^{\frac{1}{2}} (Q_1 + Q_2) D_s^{-\frac{1}{2}} \\ &= D_s^{\frac{1}{2}} Q D_s^{-\frac{1}{2}} \ . \end{aligned} \tag{66}$$

Thus, we get from (66)

$$Q = Q_1 + Q_2 \tag{67}$$

with

$$
\begin{aligned}
Q &= A^T D_{s/\tilde{\mu}} D_A^{-1} A D_s - \varkappa_0^2 D_{A\tilde{\epsilon}} + D_s^{-1} D_{A\tilde{\epsilon}} B^T D_{V\tilde{\epsilon}\tilde{\epsilon}}^{-1} B D_{A\tilde{\epsilon}} \ , \\
\tilde{Q} &= D_s^{\frac{1}{2}} A^T D_{s/\tilde{\mu}} D_A^{-1} A D_s^{\frac{1}{2}} - \varkappa_0^2 D_{A\tilde{\epsilon}} + D_s^{-\frac{1}{2}} D_{A\tilde{\epsilon}} B^T D_{V\tilde{\epsilon}\tilde{\epsilon}}^{-1} B D_{A\tilde{\epsilon}} D_s^{-\frac{1}{2}} .
\end{aligned} \tag{68}
$$

$\tilde{Q}_A$ from (64) and $\tilde{Q}$ from (65, 66, 68) are obviously symmetric matrices. Now we specify the right-hand side $\vec{r}$ introduced in (51). The discretization of the domain is demonstrated in Figure 4 with $n_x = 5$, $n_y = 4$ and $n_z = 3$.

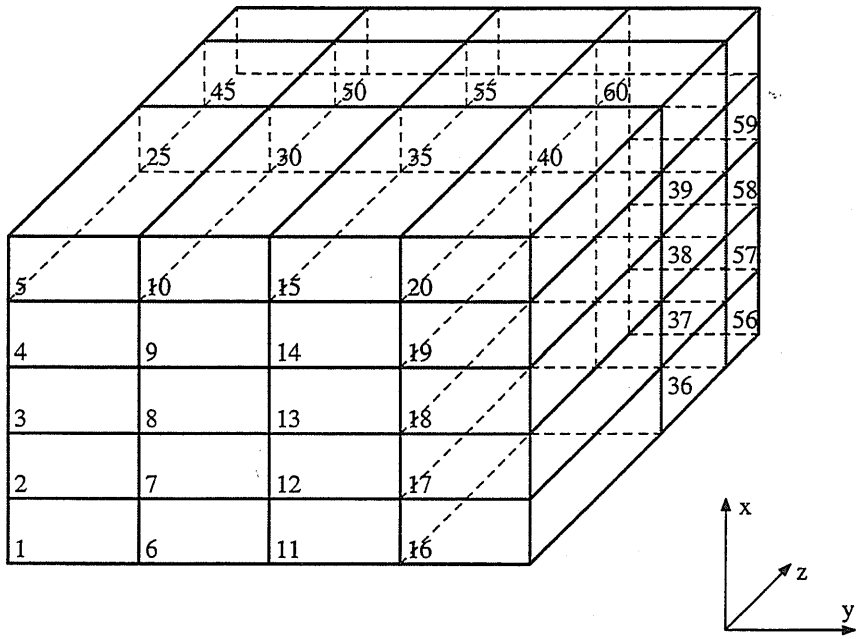

Figure 4: Decomposition of a three-dimensional domain into elementary cells

The (x, y)-coordinate plane should be the cross-sectional plane on which $E_{x_{i,j,1}}$ and $E_{y_{i,j,1}}$, $i = 1(1)n_x$, $j = 1(1)n_y$, are known solving the eigenvalue problem, that is,

$$
\begin{aligned}
e_{x_1} &= E_{x_{1,1,1}} \ , \quad e_{x_2} = E_{x_{2,1,1}} \ , \ldots , \quad e_{x_{n_{xy}}} = E_{x_{n_x,n_y,1}} \ , \\
e_{y_1} &= E_{y_{1,1,1}} \ , \quad e_{y_2} = E_{y_{2,1,1}} \ , \ldots , \quad e_{y_{n_{xy}}} = E_{y_{n_x,n_y,1}} \ .
\end{aligned} \tag{69}
$$

The elements marked by o of the matrix $\tilde{Q}_{1,r}$ (see Figure 5) are zero-elements of the matrix $\tilde{Q}_{1,A}$. These elements form the right-hand side $\vec{r}$.
The diagonal elements marked by • of the matrix $\tilde{Q}_{1,r}$ (see Figure 5) are elements of the matrix $\tilde{Q}_{1,A}$ with the value 1. These elements form also the right-hand side $\vec{r}$.

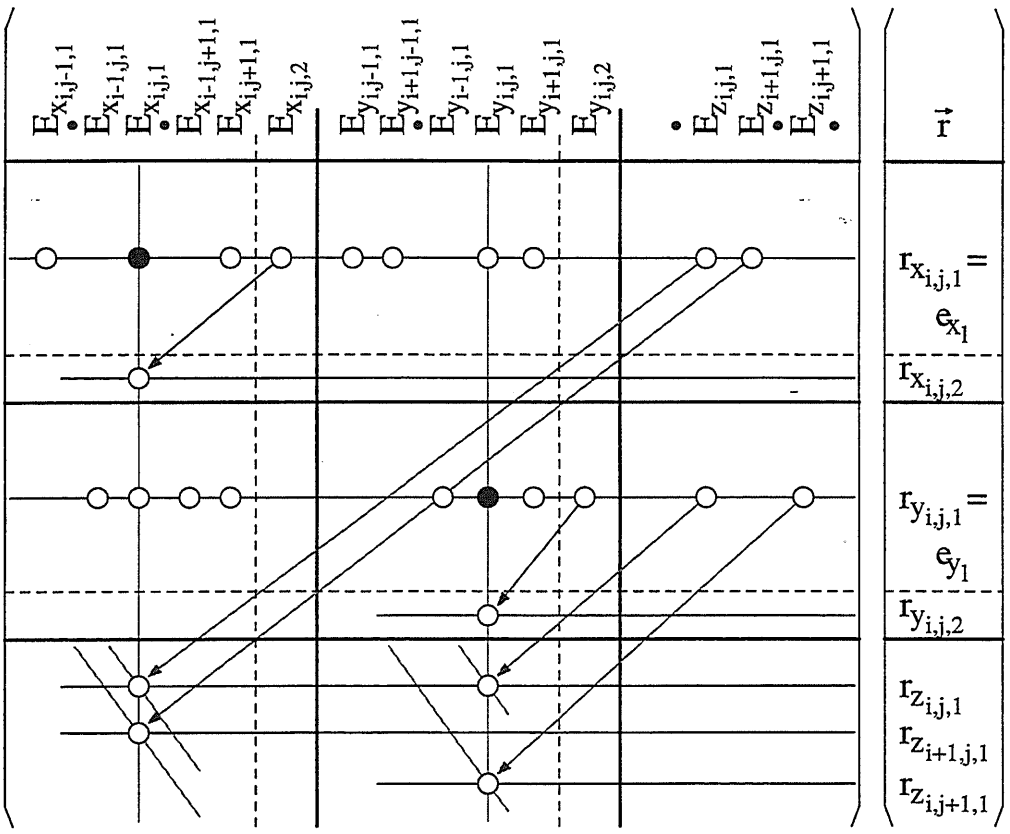

Figure 5: Topological structure of the matrix $Q_{1,r}$ and building of the right-hand side $\vec{r}$

The elements of the filled areas of the matrix $\tilde{Q}_{2,r}$ (see Figure 6) are zero-elements of the matrix $\tilde{Q}_{2,A}$.

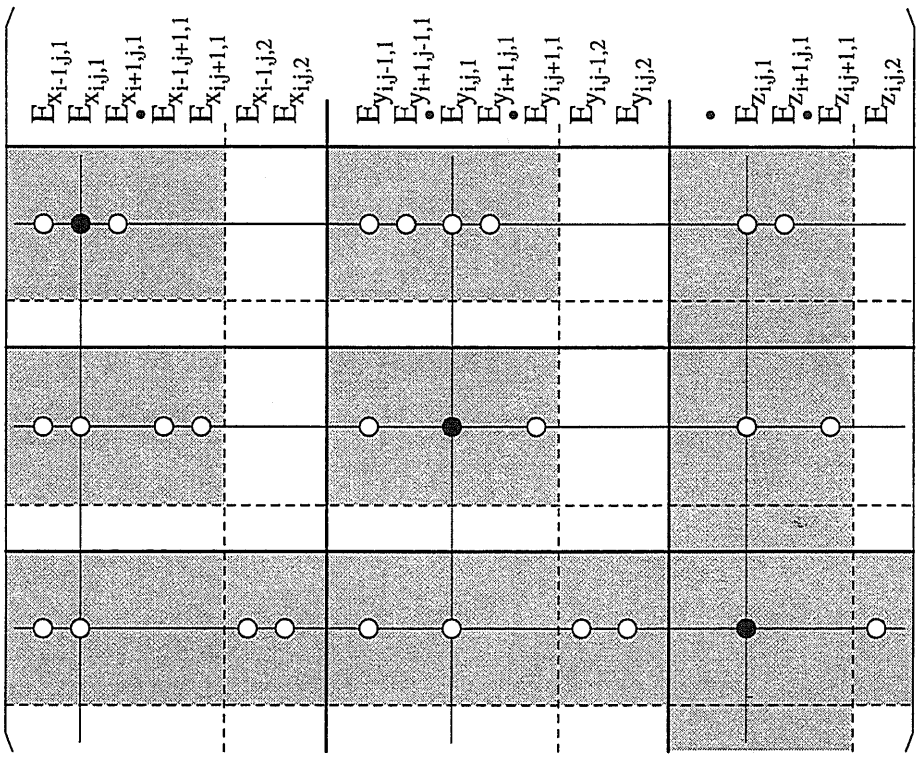

Figure 6: Topological structure of the matrix $Q_{2,r}$

Thus, we have

$$\begin{array}{llllll} \tilde{q}_{1,1} & = 1 \ , & r_{x_1} & = E_{x_{1,1,1}} & , \cdots , \\ \tilde{q}_{n_{xy},n_{xy}} & = 1 \ , & r_{x_{n_{xy}}} & = E_{x_{n_x,n_y,1}} & , \cdots , \\ \tilde{q}_{n_{xyz}+1,n_{xyz}+1} & = 1 \ , & r_{y_1} & = E_{y_{1,1,1}} & , \cdots , \\ \tilde{q}_{n_{xyz}+n_{xy},n_{xyz}+n_{xy}} & = 1 \ , & r_{y_{n_{xy}}} & = E_{y_{n_x,n_y,1}} & . \end{array} \tag{70}$$

$-c^{y,z}_{i,j,1}E_{x_{i,j,1}}$, $-c^{x,z}_{i,j,1}E_{y_{i,j,1}}$, $+c^{y,z}_{i-1,j,1}E_{x_{i-1,j,1}}$ and $+c^{x,z}_{i,j-1,1}E_{y_{i,j-1,1}}$ from (32) are known, that is,

$$r_{z_\ell} = c^{y,z}_{i,j,1}E_{x_{i,j,1}} + c^{x,z}_{i,j,1}E_{y_{i,j,1}} - c^{y,z}_{i-1,j,1}E_{x_{i-1,j,1}} - c^{x,z}_{i,j-1,1}E_{y_{i,j-1,1}} \ , \tag{71}$$

$\ell = (j-1)n_x + i$, with $i = 1, \ldots, n_x$, $j = 1, \ldots, n_y$.

Because the cross-sectional plane is located in front of the (x,y)-coordinate plane in our example, $-c^{y,z}_{i,j,1}E_{x_{i,j,1}}$ from Equation (30) and $-c^{x,z}_{i,j,1}E_{y_{i,j,1}}$ from Equation (31) for $k=2$ are known for $i=1,\ldots,n_x$ and $j=1,\ldots,n_y$, that means

$$r_{x_{n_{xy}+\ell}} = c^{y,z}_{i,j,1}E_{x_{i,j,1}}, \quad r_{y_{n_{xy}+\ell}} = c^{x,z}_{i,j,1}E_{y_{i,j,1}}, \tag{72}$$

$\ell = (j-1)n_x + i \quad \text{with} \quad i=1,\ldots,n_x, \quad j=1,\ldots,n_y.$

Generally we have to summarize the known values over all modes and all cross-sectional planes to build the right-hand side $\vec{r}$.

The magnetic-field divergence

Extracting D_A (see (39)) the matrix $\bar{B}$ (see (73)) results from (29). $\bar{B}$ consists of 3 submatrices because of homogeneity with the second Maxwellian equation. The submatrix of $\bar{B}$ is defined as the operator of the surface integral or of the divergence in the forth equation of (13) using the primary grid. The elements of $\bar{B}$ contained in a box are diagonal elements.
The following scheme gives distances between the columns which contain the diagonal element and the values 1 and -1 in the second row of $\bar{B}$. For example, n_x is the distance between the columns which correspond to $B_{y_{i,j,k}}$ and $B_{y_{i,j+1,k}}$.

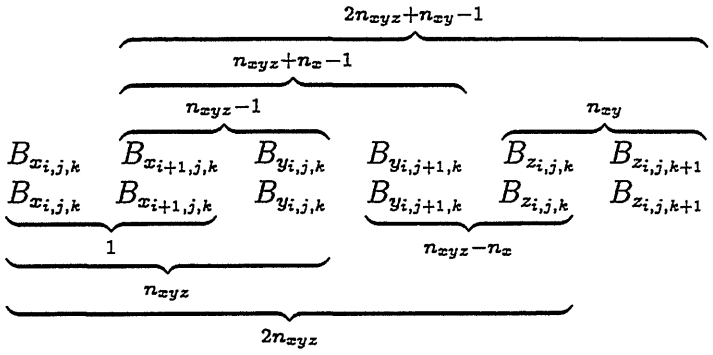

$$\bar{B} = \tag{73}$$

position	$B_{x_{i-1,j,k}}$	$B_{x_{i,j,k}}$	$B_{x_{i+1,j,k}}$	$B_{y_{i-1,j,k}}$	$B_{y_{i,j,k}}$	$B_{y_{i-1,j+1,k}}$	$B_{y_{i,j+1,k}}$	$B_{z_{i-1,j,k}}$	$B_{z_{i,j,k}}$	$B_{z_{i-1,j,k+1}}$	$B_{z_{i,j,k+1}}$
$\ell - 1$	$\boxed{1}$	-1		1		-1		1		-1	
ℓ		$\boxed{1}$	-1		1		-1		1		-1
$n_{xyz} + \ell - n_x$	1	-1		1		-1		1		-1	
$n_{xyz} + \ell$		1	-1		$\boxed{1}$		-1		1		-1
$2n_{xyz} + \ell - n_{xy}$	1	-1		1		-1		1		-1	
$2n_{xyz} + \ell$		1	-1		1		-1		$\boxed{1}$		-1

With (39) and because of $\bar{B} = B^T$ (compare (54) and (73)) we obtain the following matrix representation of the forth equation of (13):

$$\oint_{\Omega} \vec{B} \cdot d\vec{\Omega} = 0 \quad \Rightarrow \quad B^T D_A \vec{b} = 0 \ . \tag{74}$$

7 Properties of the Grid Equations

The Maxwellian grid equations are a consistent discrete representation of the analytical equations in the sense that basic properties of the analytical fields are maintained [7].
Not all of the Equations (13) are independent.

First Maxwellian equation, electric-field divergence
If the divergence of the first Maxwellian equation (see (13)) is taken, we get

$$\nabla \cdot (\nabla \times (\frac{1}{\tilde{\mu}\mu_0} \vec{B})) = \jmath\omega \nabla \cdot (\tilde{\epsilon}\epsilon_0 \vec{E}) = 0 \ , \tag{75}$$

because the divergence of the curl of any vector is identically zero. That means, we have derived for $\omega \neq 0$ the third equation of (13) from the first Maxwellian equation of (13).
The matrix representations of the first and of the third equation of (13) are (see (45) and (55), respectively)

$$A^T D_{s,\mu} \vec{b} = \jmath\omega\epsilon_0\mu_0 D_{A_{\tilde{\epsilon}}} \vec{e}, \qquad B D_{A_{\tilde{\epsilon}}} \vec{e} = 0 \ . \tag{76}$$

In order to derive the matrix representation of the electric-field divergence from the first equation in (76) we have to form the divergence in the dual grid because of (75) (see also Section 4 and Figure 3). The divergence in the dual grid is represented by the matrix B (see (54)), that means, we have to multiply the first equation of (76) with B:

$$B A^T D_{s,\mu} \vec{b} = \jmath\omega\epsilon_0\mu_0 B D_{A_{\tilde{\epsilon}}} \vec{e} \ . \tag{77}$$

BA^T in (77) is the zero matrix (for the representation of B and $A^T = \tilde{A}$ see (54) and (44), respectively):

$$B A^T \equiv 0 \ . \tag{78}$$

Hence we obtain from (77) the matrix representation of the electric-field divergence: $B D_{A_{\tilde{\epsilon}}} \vec{e} = 0$. This result is independent of the discretization size, and corresponds with (75). (77) represents the analytical identity

$$\text{div curl} \equiv 0 \ . \tag{79}$$

in the dual grid.
The analytical identity

$$\text{curl grad} \equiv 0 \tag{80}$$

is represented in the dual grid space by

$$A^T B \equiv 0 \ . \tag{81}$$

Second Maxwellian equation, magnetic-field divergence
If the divergence of the second Maxwellian equation (see (13)) is taken, we obtain

$$\nabla \cdot (\nabla \times \vec{E})) = -\jmath\omega \nabla \cdot \vec{B} = 0 \ , \tag{82}$$

because the divergence of the curl of any vector is identically zero. That means, we have derived for $\omega \neq 0$ the forth equation of (13) from the second Maxwellian equation.
The matrix representations of the second and of the forth equation of (13) are (see (41) and (74))

$$AD_s\vec{e} = -\jmath\omega D_A\vec{b}, \qquad B^T D_A\vec{b} = 0 \ . \tag{83}$$

In order to derive the matrix representation of the magnetic-field divergence from the first equation in (83) we have to form the divergence in the primary grid because of (82) (see also Section 4 and Figure 3). The divergence in the primary grid is represented by the matrix B^T (see (74)), that means, we have to multiply the first equation of (83) with B^T:

$$B^T A D_s\vec{e} = -\jmath\omega B^T D_A\vec{b} \ . \tag{84}$$

$B^T A$ in (84) is the zero matrix (for the representation of $B^T = \bar{B}$ and A see (73) and (40), respectively):

$$B^T A \equiv 0 \ . \tag{85}$$

Thus, we obtain from (84) the matrix representation of the magnetic-field divergence: $B^T D_A\vec{b} = 0$. (85) and $AB^T \equiv 0$ represent the analytical identities (79) and (80) in the primary grid space, respectively.

Remark
The relations $\bar{A} = A^T$ and $\bar{B} = B^T$ represent a topological property which is caused by the duality of the two grids.

8 The Eigenvalue Problem

The structure is shielded by an enclosure, which is assumed to be a rectangular parallelepiped. A short part of the transmission lines is considered as a part of the connecting structure, for example on the right-hand side of the cross-sectional plane $p = 1$ or the left-hand side of the cross-sectional plane $p = 2$ in Figure 1. The remaining parts of the transmission lines are located outside of the cross-sectional planes. The cross-sectional planes can be located on all faces of the enclosure, that means on the two (x, y)-, (x, z)- or (y, z)-coordinate planes. The number of transmission lines and therefore the number of cross-sectional planes on each coordinate plane can be greater than one in the model used in the program package F3D.
We consider a selected transmission line in the discussion to follow. All other transmission lines can be treated similarly. Let the z-direction be the longitudinal direction of the selected transmission line. The transmission lines are longitudinally homogeneous. Thus $\tilde{\epsilon}$ and $\tilde{\mu}$ are functions of transverse position but are independent of the longitudinal direction.

$$\begin{array}{rcccl} \tilde{\mu}_{i,j,k-1} & = & \tilde{\mu}_{i,j,k} & = & \tilde{\mu}_{i,j,k+1} \ , \\ \tilde{\epsilon}_{i,j,k-1} & = & \tilde{\epsilon}_{i,j,k} & = & \tilde{\epsilon}_{i,j,k+1} \ . \end{array} \tag{86}$$

Thus, we assume that the fields vary exponentially in the longitudinal direction:

$$\vec{E}(x, y, z \pm 2h) = \vec{E}(x, y, z) e^{\mp j k_z 2h} \ . \tag{87}$$

k_z is the propagation constant. $2h$ is the length of an elementary cell in z-direction (see (35) and Figure 7):

$$\begin{array}{rcccccccc} z_{i,j,k} & = & z_{i+1,j,k} & = & z_{i-1,j,k} & = & z_{i,j-1,k} & = & z_{i,j+1,k} & = \\ z_{i,j,k-1} & = & z_{i-1,j,k-1} & = & z_{i,j-1,k-1} & = & 2h \ . & & & \end{array} \tag{88}$$

Applying (35) and (86) to (34), we obtain

$$c^{y,x}_{i,j,k} = c^{y,x}_{i,j,k-1}, \quad c^{y,z}_{i,j,k} = c^{y,z}_{i,j,k-1} \ . \tag{89}$$

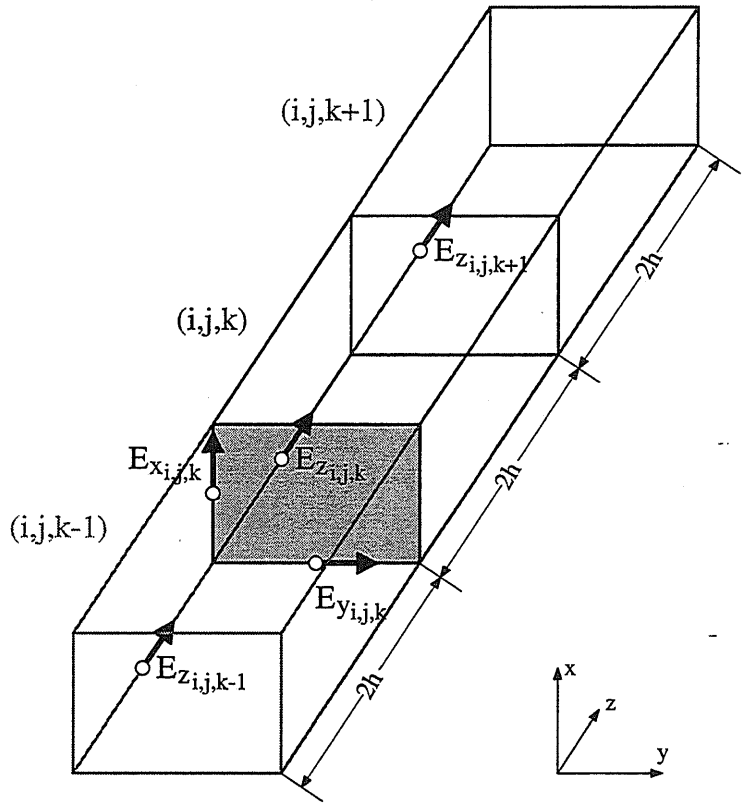

Figure 7: Reduction of the dimension

Equation (30) contains the electric field components $E_{x_{i,j,k+1}}$, $E_{z_{i,j,k-1}}$, $E_{z_{i+1,j,k-1}}$ and $E_{x_{i,j,k-1}}$. A substitution of the ansatz (87) into Equation (30) and use of (89) gives

$$c^{z,x}_{i,j,k}E_{y_{i+1,j,k}} - c^{z,y}_{i,j,k}E_{x_{i,j+1,k}} - c^{z,x}_{i,j,k}E_{y_{i,j,k}} - c^{y,x}_{i,j,k}(1 - e^{+\jmath k_z 2h})E_{z_{i,j,k}} -$$

$$c^{y,z}_{i,j,k}(e^{-\jmath k_z 2h} + e^{+\jmath k_z 2h})E_{x_{i,j,k}} + c^{y,x}_{i,j,k}(1 - e^{+\jmath k_z 2h})E_{z_{i+1,j,k}}$$

$$- c^{z,y}_{i,j-1,k}E_{x_{i,j-1,k}} - c^{z,x}_{i,j-1,k}E_{y_{i+1,j-1,k}} + c^{z,x}_{i,j-1,k}E_{y_{i,j-1,k}} +$$

$$(c^{z,y}_{i,j,k} + 2c^{y,z}_{i,j,k} + c^{z,y}_{i,j-1,k} - 2\varkappa_0^2 g^{y,z}_{i,j,k})E_{x_{i,j,k}} = 0 \ . \qquad (90)$$

The longitudinal electric field components $E_{z_{i,j,k}}$, $E_{z_{i+1,j,k}}$ in (90) can be eliminated by means of the 3rd equation in (13).
Using (87) and (see (28) and (35))

$$g^{x,y}_{i,j,k} = g^{x,y}_{i,j,k-1} \tag{91}$$

the following form of the 3rd equation of (13) yields (see (25))

$$(1 - e^{+\jmath k_z 2h})E_{z_{i,j,k}} =$$

$$-\frac{1}{g^{x,y}_{i,j,k}}(g^{y,z}_{i,j,k}E_{x_{i,j,k}} - g^{y,z}_{i-1,j,k}E_{x_{i-1,j,k}} + g^{x,z}_{i,j,k}E_{y_{i,j,k}} - g^{x,z}_{i,j-1,k}E_{y_{i,j-1,k}}) \tag{92}$$

and by index shift

$$(1 - e^{+\jmath k_z 2h})E_{z_{i+1,j,k}} =$$

$$-\frac{1}{g^{x,y}_{i+1,j,k}}(g^{y,z}_{i+1,j,k}E_{x_{i+1,j,k}} - g^{y,z}_{i,j,k}E_{x_{i,j,k}} + g^{x,z}_{i+1,j,k}E_{y_{i+1,j,k}} - g^{x,z}_{i+1,j-1,k}E_{y_{i+1,j-1,k}}) \ . \tag{93}$$

A substitution of (92) and (93) into (90) and using of

$$\gamma(h) = e^{-\jmath k_z 2h} + e^{+\jmath k_z 2h} - 2 = -4\sin^2(k_z h) \tag{94}$$

gives (95).

$$\frac{1}{c^{y,z}_{i,j,k}}(c^{y,x}_{i,j,k}g^{y,z}_{i,j,k}(\frac{1}{g^{x,y}_{i,j,k}} + \frac{1}{g^{x,y}_{i+1,j,k}}) + c^{z,y}_{i,j,k} + c^{z,y}_{i,j-1,k} - 2\varkappa_0^2 g^{y,z}_{i,j,k})E_{x_{i,j,k}} +$$

$$\frac{1}{c^{y,z}_{i,j,k}}(c^{z,x}_{i,j,k}E_{y_{i+1,j,k}} - c^{z,y}_{i,j,k}E_{x_{i,j+1,k}} - c^{z,x}_{i,j,k}E_{y_{i,j,k}}) +$$

$$\frac{c^{y,x}_{i,j,k}}{c^{y,z}_{i,j,k}}\frac{1}{g^{x,y}_{i,j,k}}(-g^{y,z}_{i-1,j,k}E_{x_{i-1,j,k}} + g^{x,z}_{i,j,k}E_{y_{i,j,k}} - g^{x,z}_{i,j-1,k}E_{y_{i,j-1,k}}) -$$

$$\frac{c^{y,x}_{i,j,k}}{c^{y,z}_{i,j,k}}\frac{1}{g^{x,y}_{i+1,j,k}}(g^{y,z}_{i+1,j,k}E_{x_{i+1,j,k}} + g^{x,z}_{i+1,j,k}E_{y_{i+1,j,k}} - g^{x,z}_{i+1,j-1,k}E_{y_{i+1,j-1,k}}) -$$

$$\frac{1}{c^{y,z}_{i,j,k}}(c^{z,y}_{i,j-1,k}E_{x_{i,j-1,k}} + c^{z,x}_{i,j-1,k}E_{y_{i+1,j-1,k}} - c^{z,x}_{i,j-1,k}E_{y_{i,j-1,k}})$$

$$= \gamma(h)E_{x_{i,j,k}} \ . \tag{95}$$

The corresponding Equation (96) is obtained from (31) in a similar way:

$$\frac{1}{c^{x,z}_{i,j,k}}(c^{x,y}_{i,j,k}g^{x,z}_{i,j,k}(\frac{1}{g^{x,y}_{i,j,k}}+\frac{1}{g^{x,y}_{i,j+1,k}})+c^{z,x}_{i,j,k}+c^{z,x}_{i-1,j,k}-2\varkappa_0^2 g^{x,z}_{i,j,k})E_{y_{i,j,k}}+$$

$$\frac{1}{c^{x,z}_{i,j,k}}(c^{z,y}_{i,j,k}E_{x_{i,j+1,k}}-c^{z,x}_{i,j,k}E_{y_{i+1,j,k}}-c^{z,y}_{i,j,k}E_{x_{i,j,k}})+$$

$$\frac{c^{x,y}_{i,j,k}}{c^{x,z}_{i,j,k}}\frac{1}{g^{x,y}_{i,j,k}}(-g^{x,z}_{i,j-1,k}E_{y_{i,j-1,k}}+g^{y,z}_{i,j,k}E_{x_{i,j,k}}-g^{y,z}_{i-1,j,k}E_{x_{i-1,j,k}})-$$

$$\frac{c^{x,y}_{i,j,k}}{c^{x,z}_{i,j,k}}\frac{1}{g^{x,y}_{i,j+1,k}}(g^{x,z}_{i,j+1,k}E_{y_{i,j+1,k}}+g^{y,z}_{i,j+1,k}E_{x_{i,j+1,k}}-g^{y,z}_{i-1,j+1,k}E_{x_{i-1,j+1,k}})-$$

$$\frac{1}{c^{x,z}_{i,j,k}}(c^{z,x}_{i-1,j,k}E_{y_{i-1,j,k}}+c^{z,y}_{i-1,j,k}E_{x_{i-1,j+1,k}}-c^{z,y}_{i-1,j,k}E_{x_{i-1,j,k}})$$

$$=\gamma(h)E_{y_{i,j,k}}\ . \tag{96}$$

Thus, the problem for the transmission line region is reduced to a two-dimensional problem, $k = const$.
We have some simplifications in the calculation of the coefficients (34), (26) and (27) because of (86) and (88). Thus we denote the terms from (34), (26), (27) and (28) with $\tilde{c}$ and $\tilde{g}$ instead of c and g, respectively, and we get

$$\begin{aligned}
\tilde{c}^{z,t}_{i,j,k} &= \frac{4h}{\tilde{\mu}_{i,j,k}t_{i,j,k}}, \quad t\in\{x,y\},\\
\tilde{c}^{s,z}_{i,j,k} &= \left(\frac{s_{i,j,k}}{\tilde{\mu}_{i,j,k}}+\frac{s_{i',j',k'}}{\tilde{\mu}_{i',j',k'}}\right)\frac{1}{2h}, \quad s\in\{x,y\},\\
\tilde{c}^{s,t}_{i,j,k} &= \left(\frac{s_{i,j,k}}{\tilde{\mu}_{i,j,k}}+\frac{s_{i',j',k'}}{\tilde{\mu}_{i',j',k'}}\right)\frac{1}{t_{i,j,k}}, \quad s,t\in\{x,y\},
\end{aligned} \tag{97}$$

and

$$\begin{aligned}
\tilde{g}^{y,z}_{i,j,k} &= h(y_{i,j,k}\tilde{\epsilon}_{i,j,k}+y_{i,j-1,k}\tilde{\epsilon}_{i,j-1,k}),\\
\tilde{g}^{x,z}_{i,j,k} &= h(x_{i,j,k}\tilde{\epsilon}_{i,j,k}+x_{i-1,j,k}\tilde{\epsilon}_{i-1,j,k}),\\
\tilde{g}^{x,y}_{i,j,k} &= (\frac{x_{i,j,k}y_{i,j,k}}{4}\tilde{\epsilon}_{i,j,k}+\frac{x_{i-1,j,k}y_{i-1,j,k}}{4}\tilde{\epsilon}_{i-1,j,k}+\\
&\quad \frac{x_{i-1,j-1,k}y_{i-1,j-1,k}}{4}\tilde{\epsilon}_{i-1,j-1,k}+\frac{x_{i,j-1,k}y_{i,j-1,k}}{4}\tilde{\epsilon}_{i,j-1,k})\ .
\end{aligned} \tag{98}$$

Taking into account the denotations (97, 98) and sorting the unknowns in (95, 96) in ascending order we obtain

$$-\frac{\tilde{c}^{z,y}_{i,j-1,k}}{\tilde{c}^{y,z}_{i,j,k}} E_{x_{i,j-1,k}} - \frac{\tilde{c}^{y,x}_{i,j,k}}{\tilde{c}^{y,z}_{i,j,k}} \frac{\tilde{g}^{y,z}_{i-1,j,k}}{\tilde{g}^{x,y}_{i,j,k}} E_{x_{i-1,j,k}} +$$

$$\left(\frac{\tilde{c}^{y,x}_{i,j,k}}{\tilde{c}^{y,z}_{i,j,k}} \left(\frac{\tilde{g}^{y,z}_{i,j,k}}{\tilde{g}^{x,y}_{i,j,k}} + \frac{\tilde{g}^{y,z}_{i,j,k}}{\tilde{g}^{x,y}_{i+1,j,k}} \right) + \frac{\tilde{c}^{z,y}_{i,j,k}}{\tilde{c}^{y,z}_{i,j,k}} + \frac{\tilde{c}^{z,y}_{i,j-1,k}}{\tilde{c}^{y,z}_{i,j,k}} - 2\varkappa_0^2 \frac{\tilde{g}^{y,z}_{i,j,k}}{\tilde{c}^{y,z}_{i,j,k}} \right) E_{x_{i,j,k}} -$$

$$\frac{\tilde{c}^{y,x}_{i,j,k}}{\tilde{c}^{y,z}_{i,j,k}} \frac{\tilde{g}^{y,z}_{i+1,j,k}}{\tilde{g}^{x,y}_{i+1,j,k}} E_{x_{i+1,j,k}} - \frac{\tilde{c}^{z,y}_{i,j,k}}{\tilde{c}^{y,z}_{i,j,k}} E_{x_{i,j+1,k}} -$$

$$\left(\frac{\tilde{c}^{y,x}_{i,j,k}}{\tilde{c}^{y,z}_{i,j,k}} \frac{\tilde{g}^{x,z}_{i,j-1,k}}{\tilde{g}^{x,y}_{i,j,k}} - \frac{\tilde{c}^{z,x}_{i,j-1,k}}{\tilde{c}^{y,z}_{i,j,k}} \right) E_{y_{i,j-1,k}} + \left(\frac{\tilde{c}^{y,x}_{i,j,k}}{\tilde{c}^{y,z}_{i,j,k}} \frac{\tilde{g}^{x,z}_{i+1,j-1,k}}{\tilde{g}^{x,y}_{i+1,j,k}} - \frac{\tilde{c}^{z,x}_{i,j-1,k}}{\tilde{c}^{y,z}_{i,j,k}} \right) E_{y_{i+1,j-1,k}} +$$

$$\left(\frac{\tilde{c}^{y,x}_{i,j,k}}{\tilde{c}^{y,z}_{i,j,k}} \frac{\tilde{g}^{x,z}_{i,j,k}}{\tilde{g}^{x,y}_{i,j,k}} - \frac{\tilde{c}^{z,x}_{i,j,k}}{\tilde{c}^{y,z}_{i,j,k}} \right) E_{y_{i,j,k}} + \left(-\frac{\tilde{c}^{y,x}_{i,j,k}}{\tilde{c}^{y,z}_{i,j,k}} \frac{\tilde{g}^{x,z}_{i+1,j,k}}{\tilde{g}^{x,y}_{i+1,j,k}} + \frac{\tilde{c}^{z,x}_{i,j,k}}{\tilde{c}^{y,z}_{i,j,k}} \right) E_{y_{i+1,j,k}}$$

$$= \gamma(h) E_{x_{i,j,k}} \ , \tag{99}$$

$$\left(-\frac{\tilde{c}^{x,y}_{i,j,k}}{\tilde{c}^{x,z}_{i,j,k}} \frac{\tilde{g}^{y,z}_{i-1,j,k}}{\tilde{g}^{x,y}_{i,j,k}} + \frac{\tilde{c}^{z,y}_{i-1,j,k}}{\tilde{c}^{x,z}_{i,j,k}} \right) E_{x_{i-1,j,k}} + \left(\frac{\tilde{c}^{x,y}_{i,j,k}}{\tilde{c}^{x,z}_{i,j,k}} \frac{\tilde{g}^{y,z}_{i,j,k}}{\tilde{g}^{x,y}_{i,j,k}} - \frac{\tilde{c}^{z,y}_{i,j,k}}{\tilde{c}^{x,z}_{i,j,k}} \right) E_{x_{i,j,k}} +$$

$$\left(\frac{\tilde{c}^{x,y}_{i,j,k}}{\tilde{c}^{x,z}_{i,j,k}} \frac{\tilde{g}^{y,z}_{i-1,j+1,k}}{\tilde{g}^{x,y}_{i,j+1,k}} - \frac{\tilde{c}^{z,y}_{i-1,j,k}}{\tilde{c}^{x,z}_{i,j,k}} \right) E_{x_{i-1,j+1,k}} + \left(-\frac{\tilde{c}^{x,y}_{i,j,k}}{\tilde{c}^{x,z}_{i,j,k}} \frac{\tilde{g}^{y,z}_{i,j+1,k}}{\tilde{g}^{x,y}_{i,j+1,k}} + \frac{\tilde{c}^{z,y}_{i,j,k}}{\tilde{c}^{x,z}_{i,j,k}} \right) E_{x_{i,j+1,k}} -$$

$$\frac{\tilde{c}^{x,y}_{i,j,k}}{\tilde{c}^{x,z}_{i,j,k}} \frac{\tilde{g}^{x,z}_{i,j-1,k}}{\tilde{g}^{x,y}_{i,j,k}} E_{y_{i,j-1,k}} - \frac{\tilde{c}^{z,x}_{i-1,j,k}}{\tilde{c}^{x,z}_{i,j,k}} E_{y_{i-1,j,k}} +$$

$$\left(\frac{\tilde{c}^{x,y}_{i,j,k}}{\tilde{c}^{x,z}_{i,j,k}} \left(\frac{\tilde{g}^{x,z}_{i,j,k}}{\tilde{g}^{x,y}_{i,j,k}} + \frac{\tilde{g}^{x,z}_{i,j,k}}{\tilde{g}^{x,y}_{i,j+1,k}} \right) + \frac{\tilde{c}^{z,x}_{i,j,k}}{\tilde{c}^{x,z}_{i,j,k}} + \frac{\tilde{c}^{z,x}_{i-1,j,k}}{\tilde{c}^{x,z}_{i,j,k}} - 2\varkappa_0^2 \frac{\tilde{g}^{x,z}_{i,j,k}}{\tilde{c}^{x,z}_{i,j,k}} \right) E_{y_{i,j,k}} -$$

$$\frac{\tilde{c}^{z,x}_{i,j,k}}{\tilde{c}^{x,z}_{i,j,k}} E_{y_{i+1,j,k}} - \frac{\tilde{c}^{x,y}_{i,j,k}}{\tilde{c}^{x,z}_{i,j,k}} \frac{\tilde{g}^{x,z}_{i,j+1,k}}{\tilde{g}^{x,y}_{i,j+1,k}} E_{y_{i,j+1,k}}$$

$$= \gamma(h) E_{y_{i,j,k}} \ . \tag{100}$$

On the transmission line wall, the tangential component of $\vec{E}$ or the tangential component of $\vec{H}$ must vanish. Hence (99) and (100) form an eigenvalue problem for the transverse electric field on the transmission line region under the boundary conditions (15). $\gamma(h)$ are the eigenvalues. $E_{x_{i,j,k}}$, $E_{y_{i,j,k}}$, $k = const$, are the components of the eigenfunctions. Solving the eigenvalue problem the transverse electric fields $\vec{E}^{(p)}_{t,l}$, $l = 1(1)m^{(p)}$, are known at

the cross-sectional planes p, and the boundary condition (14) can be build superposing the transmission line modes $\vec{E}_{t,l}^{(p)}$, $l = 1(1)m^{(p)}$, with weighted mode-amplitude sums (see [4]).
If the cross-sectional plane is located on the (x,z)-plane of the enclosure, we can develop in a similar way the equations which correspond to (99) and (100).
We get formally the corresponding equations if we change the variable y to z and shift the indices j to k and k to j, $j = const.$
The same can be performed for the (y,z)-plane of the enclosure.

9 Conclusion

The model for the simulation of monolithic microwave integrated circuits, and the finite-volume method for the solution of the corresponding three-dimensional boundary value problem for the Maxwellian equations has been presented. The application of the finite-volume method results in an eigenvalue problem for nonsymmetric matrices and the solution of a system of linear equations with indefinite symmetric matrices.
Improved numerical solutions for this two time- and memory-consuming linear algebraic problems, the computation of the scattering matrix and of the used orthogonality relation are treated in [4].

References

[1] Beilenhoff, K., Heinrich, W., Hartnagel, H. L., *Improved Finite-Difference Formulation in Frequency Domain for Three-Dimensional Scattering Problems*, IEEE Transactions on Microwave Theory and Techniques, Vol. 40, No. 3, March 1992.

[2] Christ, A., Hartnagel, H. L., *Three-Dimensional Finite-Difference Method for the Analysis of Microwave-Device Embedding*, IEEE Transactions on Microwave Theory and Techniques, Vol. MTT-35, No. 8, pp. 688-696, June 1987.

[3] Christ, A., *Streumatrixberechnung mit dreidimensionalen Finite-Differenzen für Mikrowellen-Chip-Verbindungen und deren CAD-*

Modelle, Fortschrittberichte VDI, Reihe 21: Elektrotechnik, Nr. 31, 1-154, 1988.

[4] Hebermehl, G., Schlundt, R., Zscheile, H., Heinrich, W., *Improved Numerical Solutions for the Simulation of Monolithic Microwave Integrated Circuits*, Preprint No. 236, Weierstraß-Institut für Angewandte Analysis und Stochastik im Forschungsverbund Berlin e.V., 1996.

[5] Weiland, T., *Zur numerischen Lösung des Eigenwellenproblems längshomogener Wellenleiter beliebiger Randkontur und transversal inhomogener Füllung*, Dissertation, Fachbereich 17 der Technischen Hochschule Darmstadt, 1977.

[6] Weiland, T., *Eine numerische Methode zur Lösung des Eigenwellenproblems längshomogener Wellenleiter*, AEÜ, Band 31, Heft 7/8, 308-314, 1977.

[7] Weiland, T., *Time Domain Electromagnetic Field Computation with Finite Difference Methods*, Second International Workshop on Discrete Time Domain, Modeling of Electromagnetic Fields and Networks, Berlin, Hotel Ambassador, 28./29. October 1993.

[8] Yee, K. S., *Numerical Solution of Initial Boundary Value Problems Involving Maxwell's Equations in Isotropic Media*, IEEE Transactions on Antennas and Propagation, Vol. AP-14, No. 3, May 1966.

Recent publications of the Weierstraß–Institut für Angewandte Analysis und Stochastik

Preprints 1995

206. Wolfgang Dahmen, Angela Kunoth, Reinhold Schneider: Operator equations, multiscale concepts and complexity.

207. Annegret Glitzky, Konrad Gröger, Rolf Hünlich: Free energy and dissipation rate for reaction diffusion processes of electrically charged species.

208. Jörg Schmeling: A dimension formula for endomorphisms – The Belykh family.

209. Alfred Liemant: Leitfähigkeit eindimensionaler periodischer elektrischer Netze.

210. Günter Albinus: A thermodynamically motivated formulation of the energy model of semiconductor devices.

211. Dmitry Ioffe: Extremality of the disordered state for the Ising model on general trees.

212. Stefan Seelecke: Equilibrium thermodynamics of pseudoelasticity and quasi-plasticity.

Preprints 1996

213. Björn Sandstede: Stability of N–fronts bifurcating from a twisted heteroclinic loop and an application to the FitzHugh–Nagumo equation.

214. Jürgen Sprekels, Songmu Zheng, Peicheng Zhu: Asymptotic behavior of the solutions to a Landau–Ginzburg system with viscosity for martensitic phase transitions in shape memory alloys.

215. Yuri I. Ingster: On some problems of hypothesis testing leading to infinitely divisible distributions.

216. Grigori N. Milstein: Evaluation of moment Lyapunov exponents for second order linear autonomous SDE.

217. Hans Günter Bothe: Shift spaces and attractors in non invertible horse shoes.

218. Gianfranco Chiocchia, Siegfried Prößdorf, Daniela Tordella: The lifting line equation for a curved wing in oscillatory motion.

219. Pavel Krejčí, Jürgen Sprekels: On a system of nonlinear PDE's with temperature–dependent hysteresis in one–dimensional thermoplasticity.

220. Boris N. Khoromskij, Siegfried Prößdorf: Fast computations with the harmonic Poincaré–Steklov operators on nested refined meshes.

221. Anton Bovier, Véronique Gayrard: Distribution of overlap profiles in the one–dimensional Kac–Hopfield model.

222. Jürgen Sprekels, Dan Tiba: A duality–type method for the design of beams.

223. Wolfgang Dahmen, Bernd Kleemann, Siegfried Prößdorf, Reinhold Schneider: Multiscale methods for the solution of the Helmholtz and Laplace equation.

224. Herbert Gajewski, Annegret Glitzky, Jens Griepentrog, Rolf Hünlich, Hans–Christoph Kaiser, Joachim Rehberg, Holger Stephan, Wilfried Röpke, Hans Wenzel: Modellierung und Simulation von Bauelementen der Nano– und Optoelektronik.

225. Andreas Rathsfeld: A wavelet algorithm for the boundary element solution of a geodetic boundary value problem.

226. Sergej Rjasanow, Wolfgang Wagner: Numerical study of a stochastic weighted particle method for a model kinetic equation.

227. Alexander A. Gushchin: On an information–type inequality for the Hellinger process.

228. Dietmar Horn: Entwicklung einer Schnittstelle für einen DAE–Solver in der chemischen Verfahrenstechnik.

229. Oleg V. Lepski, Vladimir G. Spokoiny: Optimal pointwise adaptive methods in nonparametric estimation.

230. Bernd Kleemann, Andreas Rathsfeld, Reinhold Schneider: Multiscale methods for boundary integral equations and their application to boundary value problems in scattering theory and geodesy.

231. Jürgen Borchardt, Ludger Bruell, Friedrich Grund, Dietmar Horn, Frank Hubbuch, Tino Michael, Horst Sandmann, Robert Zeller: Numerische Lösung großer strukturierter DAE–Systeme der chemischen Prozeßsimulation.

232. Herbert Gajewski, Klaus Zacharias: Global behaviour of a reaction–diffusion system modelling chemotaxis.

233. Fréderic Guyard, Reiner Lauterbach: Forced symmetry breaking perturbations for periodic solutions.

234. Vladimir G. Spokoiny: Adaptive and spatially adaptive testing of a nonparametric hypothesis.